Materials Science and Engineering C 59 (2016) 1143–1167

Contents lists available at ScienceDirect

Materials Science and Engineering C

journal homepage: www.elsevier.com/locate/msec

Review

Structure and mechanical properties of selected protective systems in marine organisms

Steven E. Naleway [a,*], Jennifer R.A. Taylor [b], Michael M. Porter [e], Marc A. Meyers [a,c,d], Joanna McKittrick [a,c]

[a] Materials Science and Engineering Program, University of California, San Diego, La Jolla, CA 92093, USA
[b] Scripps Institution of Oceanography, University of California, San Diego, La Jolla, CA 92037, USA
[c] Department of Mechanical and Aerospace Engineering, University of California, San Diego, La Jolla, CA 92093, USA
[d] Department of NanoEngineering, University of California, San Diego, La Jolla, CA 92093, USA
[e] Department of Mechanical Engineering, Clemson University, Clemson, SC 29634, USA

ARTICLE INFO

Article history:
Received 21 January 2015
Received in revised form 29 September 2015
Accepted 12 October 2015
Available online 23 October 2015

Keywords:
Marine organisms
Protective mechanisms
Structural biological materials
Bioinspired design

ABSTRACT

Marine organisms have developed a wide variety of protective strategies to thrive in their native environments. These biological materials, although formed from simple biopolymer and biomineral constituents, take on many intricate and effective designs. The specific environmental conditions that shape all marine organisms have helped modify these materials into their current forms: complete hydration, and variation in hydrostatic pressure, temperature, salinity, as well as motion from currents and swells. These conditions vary throughout the ocean, being more consistent in the pelagic and deep benthic zones while experiencing more variability in the nearshore and shallows (e.g. intertidal zones, shallow bays and lagoons, salt marshes and mangrove forests). Of note, many marine organisms are capable of migrating between these zones. In this review, the basic building blocks of these structural biological materials and a variety of protective strategies in marine organisms are discussed with a focus on their structure and mechanical properties. Finally, the bioinspired potential of these biological materials is discussed.

Contents

* Corresponding author.
E-mail addresses: snaleway@eng.ucsd.edu (S.E. Naleway), j3taylor@ucsd.edu (J.R.A. Taylor), mmporte@clemson.edu (M.M. Porter), mameyers@eng.ucsd.edu (M.A. Meyers), jmckittrick@eng.ucsd.edu (J. McKittrick).

http://dx.doi.org/10.1016/j.msec.2015.10.033
0928-4931/

1. Introduction

The study of biological materials within materials science provides the nexus where the fields of physics, engineering, chemistry and biology converge to understand and harness the vast body of knowledge that can be learned from the natural world. The findings of this research provide for better biological understanding of the complex and unique organisms and structures in nature. In addition, this knowledge provides inspiration for the peripheral fields of bioinspired materials, where synthetic structures are inspired by nature, and biomaterials, where materials and structures are designed for optimum compatibility with biological systems.

While still bound by the same physical laws, biological materials are starkly different from synthetic ones. To succinctly describe the unique qualities of biological materials, seven interrelated features have been identified (inspired by Arzt [1] and expanded by Meyers et al. and Chen et al. [2–5]). These characteristics are: self-assembly, multifunctionality, hierarchical design, hydration effects, mild synthesis conditions, evolutionary design and environmental constraints, and self-healing capability. While they apply throughout biology, marine organisms face a number of specific environmental constraints not shared by their terrestrial counterparts. These marine specific conditions include: complete hydration, and variation in hydrostatic pressure (0.1–100 MPa), temperature (−2–38 °C), salinity (34–36 ppt), as well as motion from currents and swells. These conditions vary throughout the ocean, being more consistent in the pelagic and deep benthic zones while experiencing more variability in the nearshore and shallows (e.g. intertidal zones, shallow bays and lagoons, salt marshes and mangrove forests). Of note, many marine organisms are capable of migrating between these zones, forcing them to be dynamic through many environments. Through evolution, these environmental constraints have shaped the form of all structural marine biological materials.

The combination of these qualities provides for high levels of complexity and performance within marine biological materials. This is enacted through hierarchical structural design elements [6]. The toughness of biological materials and their constituents is plotted as a function of the elastic modulus in Fig. 1. The high toughness of biopolymers together with the high strength of biominerals is combined into many composite biological materials (e.g. bone and mollusk shell) [7]. When compared to engineered synthetic materials, metals and ceramics are capable of providing mechanical properties up to an order of magnitude higher than biological materials. However, biominerals (natural ceramics) and biopolymers (natural polymers) are mechanically comparable with many synthetic engineering composites and engineering polymers, respectively [5].

Biological materials can be systematized along different classification methods. Naleway et al. [6] recently proposed eight structural design elements as a new paradigm for identifying common features in different organisms. Using a similar methodology, the organisms and structures in this manuscript can be divided into four classes based upon their biomechanical function:

1. Crushing resistant structures: found within the exoskeletons of mollusks, crustaceans, diatoms and coccolithophores, and the skeletal armor of the seahorse.
2. Flexure resistant structures: found within sea sponge spicules, the spines of sea urchins and porcupine fish.
3. Piercing resistant structures: found within the scales and scutes of fish as well as marine skeletal armors.
4. Impact resistant structures: found in the dactyl clubs of the mantis shrimp.

There are protective structures that provide effective resistance to multiple forms of stress, however here we aim to highlight the most

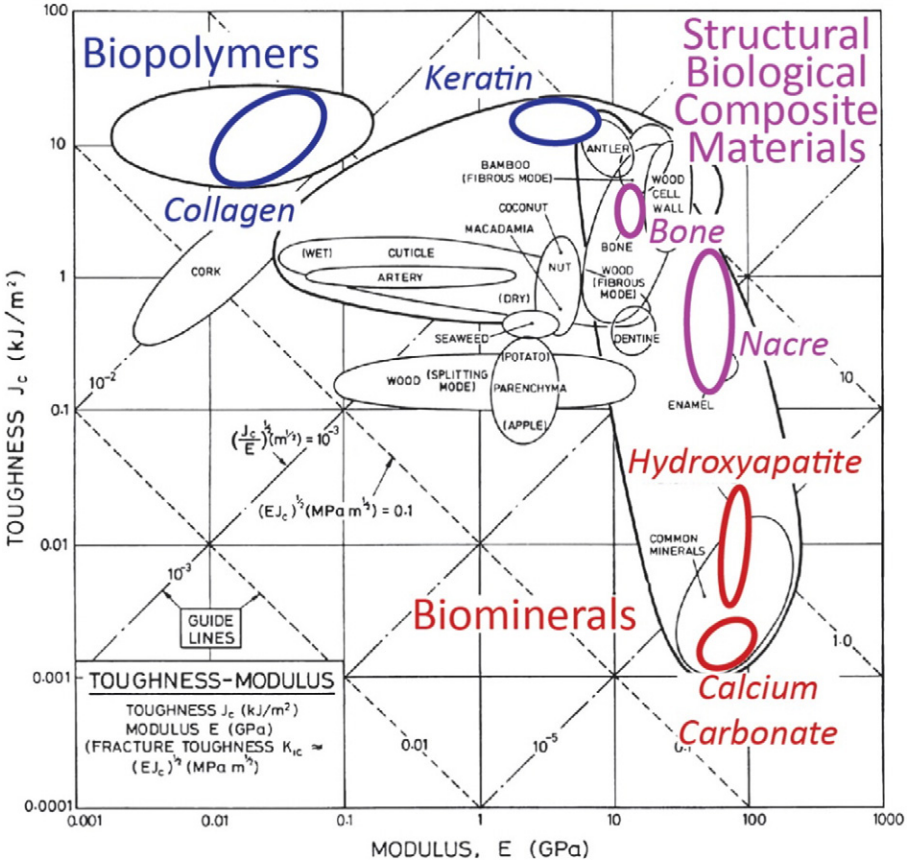

Fig. 1. Toughness as a function of elastic modulus for biological materials.
Adapted from [7].

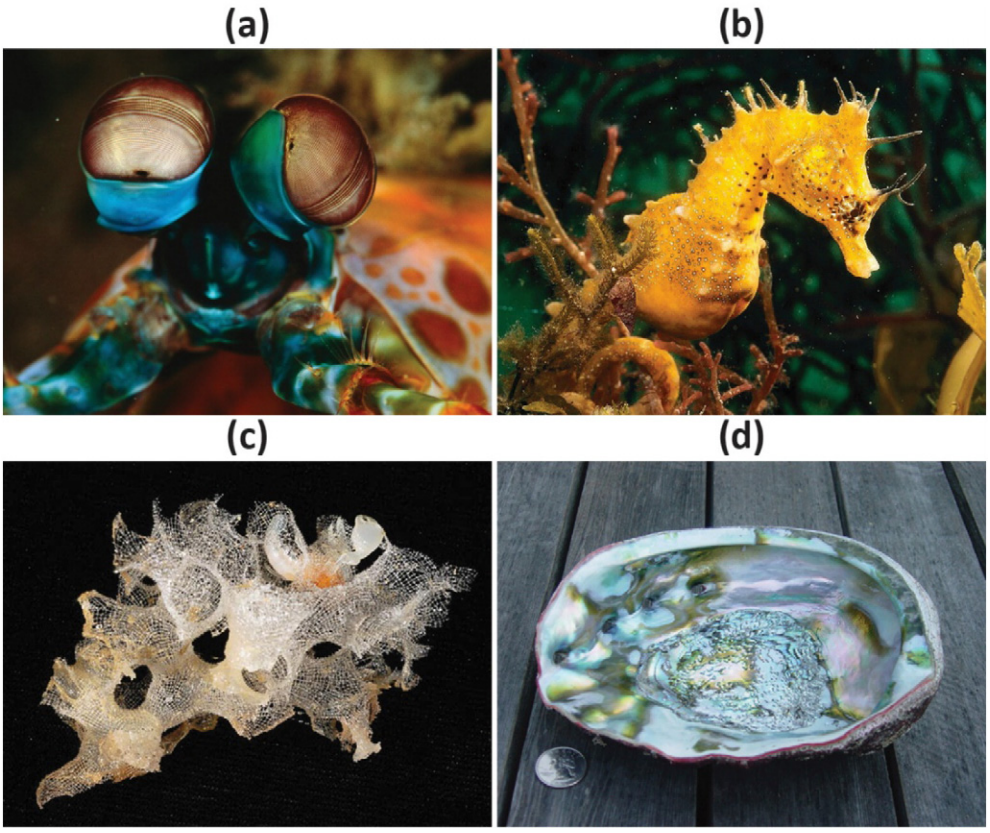

Fig. 2. Examples of some spectacular marine organisms. (a) *Odontodactylus* (mantis shrimp); (b) *Hippocampus* (seahorse); (c) *Farrea* (honeycomb glass sponge); (d) *Haliotis* (abalone). Adapted from: (a)–(c) nationalgeographic.com, (d) wikipedia.com.

remarkable defenses of individual organisms. We describe notable examples of organisms within each of these classes focusing primarily on systems that have a protective exoskeleton, or shell, that surrounds a soft body. The approach used here provides a valuable perspective on how the materials science methodology, connecting the structure (at various levels, from nano- to macro-) and mechanical properties, can enhance our understanding of nature and guide us to novel bio-inspired designs.

Recent analysis suggests that ~2.2 million of the world's ~8.7 million eukaryotic species reside within the oceans and that 91% of these marine species have yet to be discovered and catalogued [8]. These organisms (Fig. 2 shows some examples) offer an amazing array of traits and properties due to the design of their complex biological materials. The lessons learned from the structural biological materials of marine organisms have stimulated a number of bioinspired designs including high toughness materials inspired by abalone nacre [9], fiber optic wires inspired by sea sponge spicules [10,11] and body armor inspired by fish scales [12,13]. Given the complex structures that have already been discovered and the immense number of organisms that have yet to be investigated, the study of structural biological materials of marine organisms offers much interest to the scientific community.

2. Basic building blocks of marine organisms

While there is a large variety of marine biological materials, the building blocks of these structures are quite simple. These consist of two basic classes: biopolymers (collagen, keratin and chitin) and biominerals (hydroxyapatite, calcium carbonate and amorphous silica being the principal ones). While these materials are simple, they are combined in a significant level of complexity. This can often allow for mechanical performance which exceeds that of the individual constituents [9]. Focusing on marine organisms, the mechanical properties of

Table 1
Mechanical properties of marine biological material constituents.

Material	Elastic modulus (E) (GPa)	UCS[a] (MPa)	UTS[b] (MPa)	Example biological organisms	Reference
Biopolymer constituents					
Type I collagen	0.05–1		20–100	Fish scales	[30,217,218]
Chitin	1–20		200	Mollusk and crab exoskeletons	[219]
Keratin	0.1–5		60–200	Hagfish slime, squid beaks	[30]
Biomineral constituents					
Hydroxyapatite	50–112	30–115		Fish scales	[217,218,220]
Calcium carbonate	50–150	100–200		Mollusk and crab exoskeletons, sea urchin spines	[7]
Amorphous silica	60–75		155–200[c]	Sea sponge spicules, diatom exoskeletons	[221,222]
Magnetite	72			Chiton teeth	[223]

[a] Ultimate compressive strength.
[b] Ultimate tensile strength.
[c] Values taken in 3-point bending mode.

biological material constituents (Table 1) and a variety of biological materials (Table 2) are highlighted. The wide range of strengths and moduli that marine organisms employ in their biological materials in order to best thrive in their environment are shown in Tables 1 and 2.

In general, there are two basic forms of biological materials: (1) non-mineralized biological materials that consist of only biopolymers and usually take the form of directionally aligned fibers (e.g. aligned in parallel or helical patterns such as Bouligand configurations) and (2) mineralized biological materials which are composites composed of both biopolymers and biominerals arranged into hierarchical structures. In this review we focus upon protective and/or load bearing structural biological materials, most of which are mineralized.

The combination of high compressive strength of biominerals and high toughness of biopolymers is the key to incorporating these generally mutually exclusive properties (strength and toughness) [14] into many structural biological materials. The balance between these properties has been shown to relate to the mineral content where an increase relates to an increase in strength and elastic modulus with an accompanying decrease in toughness [15]. Table 3 displays the relative proportions of these phases in structural biological materials of marine organisms. Additionally, mammalian bone and human dentin are displayed for reference.

2.1. Biopolymers

Biopolymers make up the compliant phase in structural biological materials. In marine structural biological materials, the principal biopolymers are collagen, keratin and chitin. Collagen-based cartilage is also present in some marine organisms. Generally fibrous in nature, these structures can be highly anisotropic and tend to display varying mechanical properties depending upon their arrangement, alignment and organization. Additionally, they are generally stronger in tension than compression.

Collagen is one of the most important biopolymers found throughout the metazoan diversity and is the basic component in skin, tendon, bone and cartilage [2,16]. While there are no fewer than 29 different collagen types, the majority of collagen found in organisms (~90% of collagen found in the human body) is type I collagen [16]. Within marine organisms, type I collagen has been extracted from the tissue of sea urchins [17,18], octopus [19], starfish [20], jellyfish [21,22] and a number of fish species [23–25].

Type I collagen takes the form of fibers and displays four levels of hierarchy from the molecular- to macro-level (Fig. 3) [16]. At the molecular level, triple helix segments (Fig. 3a) assemble into tropocollagen molecules (Fig. 3b) that further assemble into collagen fibrils exhibiting diameters of 50–200 nm (Fig. 3c) [26] that finally agglomerate into collagen fibers with diameters of 0.5 to 3 μm (Fig. 3d) [16]. The offset of the tropocollagen molecules, diagramed in Fig. 3c and imaged on collagen fibrils from a fish scale through atomic force microscopy (AFM) in Fig. 3e, creates a characteristic banding, periodically spaced at 67 nm, on the collagen fibrils [3,26–29].

Given their fibrous nature, the mechanical properties of collagen-based materials are highly anisotropic. Collagen structures tend to be highly oriented in order to provide optimized strength and mechanical properties along specific directions [7]. Collagen also often serves as a basic structural template for biomineralization [28].

Keratin is an integral element in the outer covering of many vertebrates and is commonly found in skin, hair, nails, beaks, turtle shells and hagfish slime [30–32]. There are two types of keratin: α-keratin (Fig. 4a) that forms in helices and β-keratin (Fig. 4b) that forms in

Table 2
Mechanical properties of selected marine biological materials tested in a quasi-static, hydrated state.

Biological material	Elastic modulus (*E*) (GPa)	UCS[a] (MPa)	UTS[b] (MPa)	Reference
Abalone shell (nacre)	60	235–540	140	[102,224]
Crab exoskeleton (leg)	0.47–0.52	57	30–31.5	[133,143,144]
Crab exoskeleton (claw)	4.9			[142]
Mantis shrimp dactyl club	75			[204]
Fish scale (*Pagrus major*)	2.2		93	[64]
Diatom exoskeleton	22.4	330–680	155–560	[121]
Sea urchin spines	21	42–49		[163,168]
Conch shell	30	180–310		[104]
Hagfish slime	0.006		180	[225]
Sea sponge spicules	36–38		593–880[c]	[221,222]

[a] Ultimate compressive strength.
[b] Ultimate tensile strength.
[c] Values taken in 3-point bending mode.

Table 3
Relative weight proportions of biomineral and biopolymer constituents for marine organisms.

Organism (sample type)	Ratio of biomineral: biopolymer (by weight)	Reference
Snow crab (claw)	3.8:1	[133]
Snow crab (carapace)	1.6:1	[133]
American lobster (carapace)	1.7:1	[226]
Cod (clythrum bone)	6.4:1	[227]
Seahorse (bony plates)	1.5:1	[150]
Red abalone (shell)	19:1	[96]
Sea sponge (spicules)	3:1	[82]
Red seabream (fish scales)	1:1.2	[64]
Barramundi (fish scales)	1:1.5	[228]
Longhorn cowfish (fish scales)	1:2	[12]
Cow (femur bone)	2.6:1	[52]
Human (dentin)	1.8:1	[4]

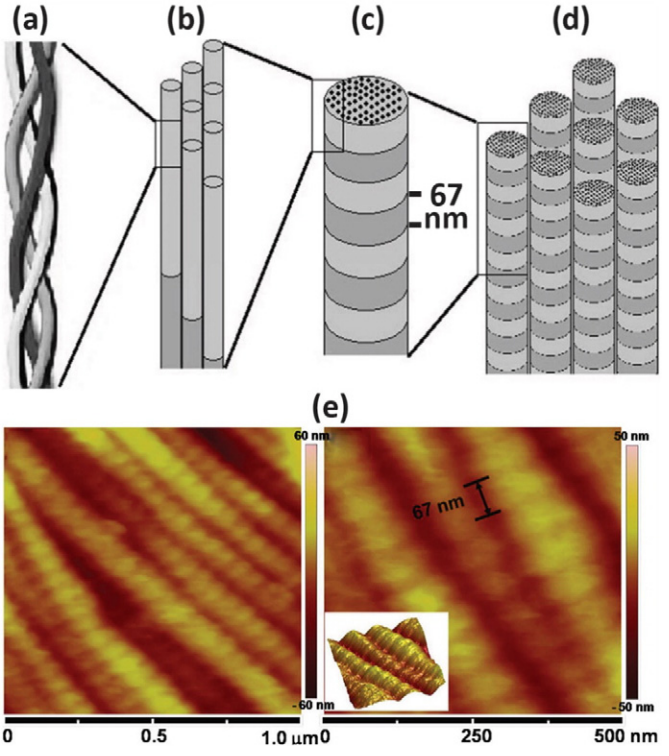

Fig. 3. Diagram of the hierarchical structure of collagen fibers. (a) Triple helix segments; (b) tropocollagen molecules; (c) assembled collagen fibrils with the characteristic periodic 67 nm spacing highlighted; (d) collagen fibers assembled from multiple collagen fibrils; (e) atomic force micrograph of a collagen fibril from fish scales with the characteristic spacing highlighted.
Adapted from: (a)–(d) [16], (e) [29].

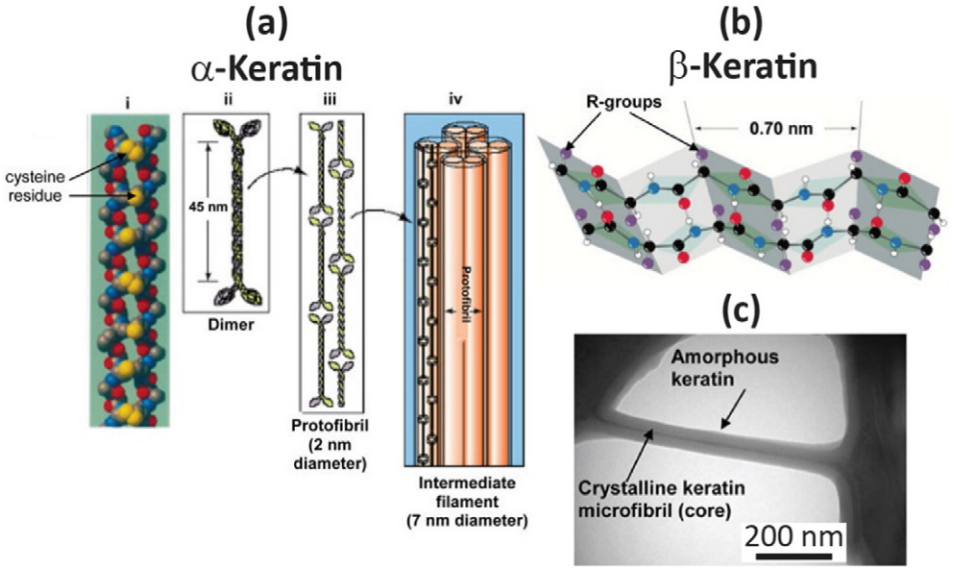

Fig. 4. Structure of keratin. (a) Hierarchy of α-keratin showing the assembly from two polypeptide chains (i) to a fibrous structure (iv); (b) β-keratin that shows a pleated sheet shape that consists of antiparallel chains with R-groups that extend between sheets; (c) TEM micrograph of α-keratin from a sheep horn that displays the composite structure of a crystalline keratin core within an amorphous keratin matrix.
Adapted from: (a) [30,209], (b) [30], (c) [30,210].

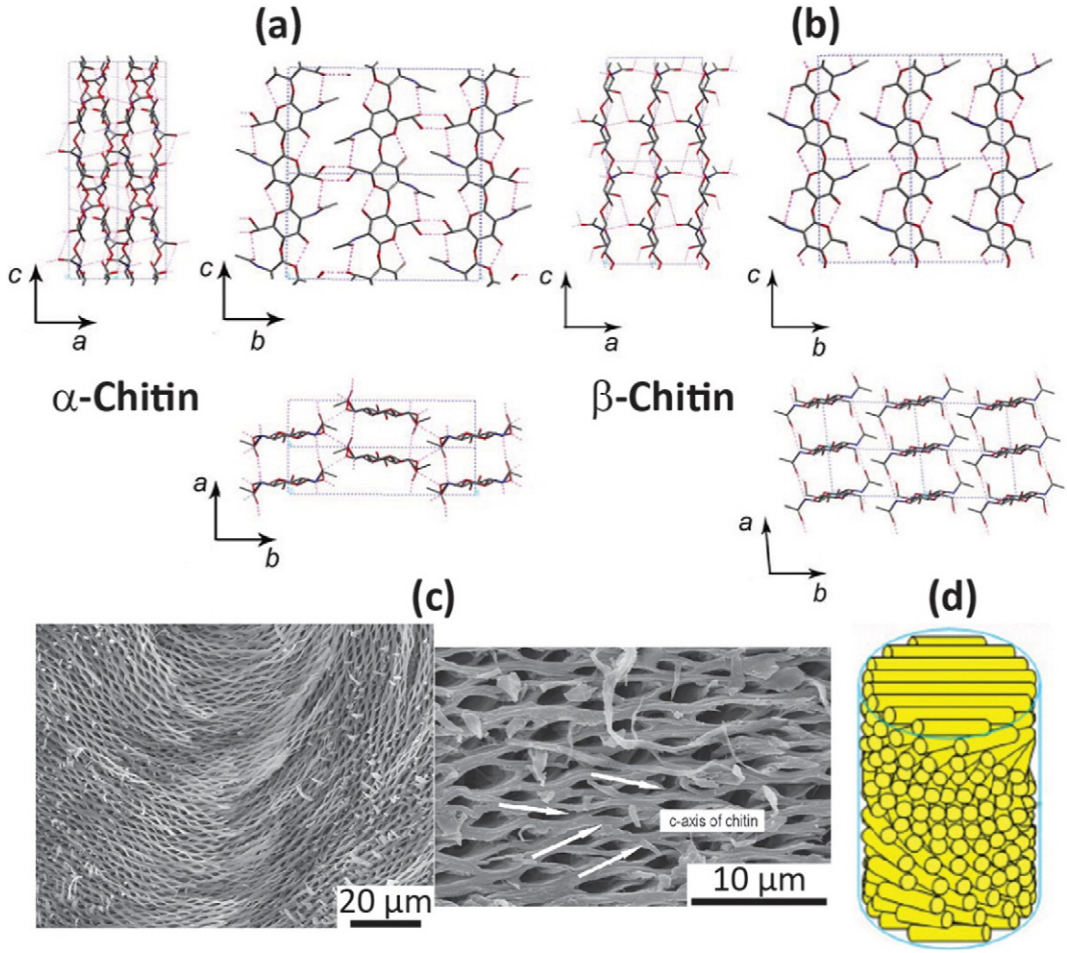

Fig. 5. Diagram of the structure of chitin. (a) The molecular structure of α-chitin viewed from three different directions; (b) the molecular structure of β-chitin viewed from three different directions; (c) aligned microstructure of mineralized α-chitin fibers from the exoskeleton of a lobster; (d) diagram of the helical Bouligand structure of many chitin materials, such as crustacean exoskeletons.
Adapted from: (a) and (b) [41], (c) [211], (d) [4].

pleated sheets [30]. The fibrous structure of α-keratin is similar to type I collagen as both consist of hierarchically assembled molecules, two polypeptide chains in α-keratin (Fig. 4a) and three tropocollagen molecules for type I collagen (Fig. 3a). However, once the cells that produce keratin (keratinocytes) assemble, they die, resulting in a non-vascularized "dead" tissue that is in contrast to the extracellular "living" matrix of collagen, into which live cells are embedded [30]. Additionally, keratin can be considered a composite material, similar to synthetic semi-crystalline polymers, consisting of fibers of crystalline keratin reinforcing an amorphous keratin matrix (Fig. 4c) [33]. While they have different forms, both α-keratin and β-keratin have similar numbers of polypeptide chains, suggesting that they both originate from the same microfibril structure [34]. Within marine biological materials α-keratin is much more common than β-keratin.

Quite similar to type I collagen, the mechanical properties of fibrous α-keratin are highly anisotropic [35,36]. Given this alignment, α-keratin is capable of much higher mechanical properties parallel to the fiber direction than the more isotropic β-keratin [30]. Additionally, the composite nature of keratin results in a roughly inverse relationship between the stiffness (elastic modulus) and the volume fraction of amorphous matrix (less-crystalline composite) (i.e. as the content of the amorphous keratin increases, the bulk keratin's stiffness decreases) [30,37]. This relationship between crystallinity and elastic modulus is also common to semi-crystalline synthetic polymers [38,39].

Chitin is found throughout a number of organisms and is the most abundant natural polysaccharide [40]. In marine biological materials it is mainly associated with the exoskeletons of marine crustaceans and mollusks and the beaks of squids and octopuses [40–42]. In squid beaks, chitin is cross-linked (also known as sclerotization or tanning) with proteins, forming a tough material despite lacking biominerals [42]. Two main varieties of chitin, α-chitin and β-chitin (Fig. 5a–b), are commonly present in organisms, with α-chitin being the most abundant. Specifically, α-chitin is characteristic of crustacean exoskeletons (Fig. 5c) [28] while β-chitin is found in the pens of squid (the internal rigid structural element that supports the squid's mantle) [43] and the spines of diatoms. β-Chitin is less crystalline than the more common α-chitin and is metastable, being able to transform into stable α-chitin if induced by the intercalation of molecules into its lattice [28]. Chitin chains are hierarchically organized into fibers of more than 1 μm in diameter [28].

While chitin itself is often in a fibrous form, in most organisms it is aligned in helicoidal planes to form a twisted plywood or Bouligand structure (Fig. 5d) [4,44–47]. This structure provides for more in-plane isotropy, allowing for the use of relatively un-mineralized chitin in squid pens and crustacean exoskeletons while still maintaining strength and toughness [4].

Cartilage is generally an internal support structure in organisms and is comprised of a number of fibrous proteins (collagens) along with polysaccharides and peptides [48]. Cartilage can be either mineralized or non-mineralized and is most commonly associated with internal structures such as the skeletons of sharks, rays and chimaeras [49]. However, it is found within a number of mollusks, including cephalopods (e.g. squid) and gastropods (e.g. snails), generally within their fleshy tissues [50,51]. Mechanically, cartilage is a viscoelastic material that is highly variable in strength depending upon the level of mineralization [48].

2.2. Biominerals

Biominerals compose the rigid phase of structural biological materials. Biological composites are generally formed through biomineralization of biopolymer templates with minerals, primarily hydroxyapatite, calcium carbonate and silica [28]. However, magnetite (Fe_3O_4) and iron sulfide (FeS) are also found within a select number of organisms [3].

Non-stoichiometric hydroxyapatite ($Ca_{10}(PO_4)_6(OH)_2$), where 4–6% of the phosphate groups are replaced by carbonate groups [52], constitutes the biomineral phase of bone, teeth and most fish scales [13, 53–56]. Given its presence in the bones and teeth of humans, it has garnered a significant amount of research in the biomedical field, producing a number of bioinspired designs with a focus on biomedical materials and implants [9,57–61]. Biogenic hydroxyapatite often forms around a collagen scaffold that directs growth (Fig. 6a) [62]. As shown in Fig. 6b–c for fish scales, this causes the hydroxyapatite to take on

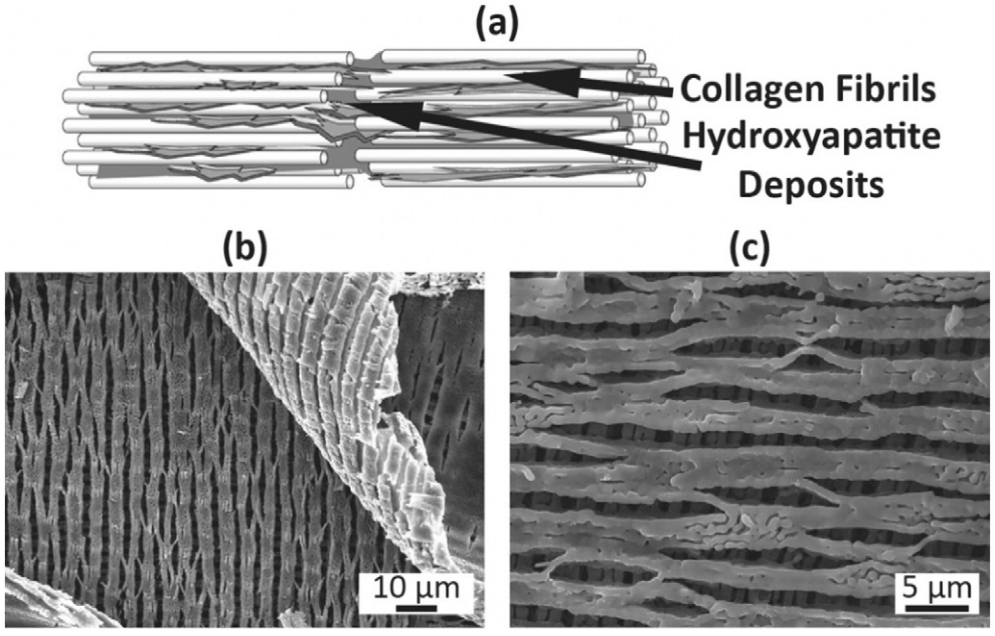

Fig. 6. Growth and structure of hydroxyapatite and, in the case of bone, carbonated hydroxyapatite. (a) A diagram of the biomineralization of hydroxyapatite where collagen (or other biopolymer) fibrils template hydroxyapatite crystal growth; deproteinized tissue (by heating at 1473 K, images of tissue from a sea bream (*Pagrus major*)) at (b) low and (c) high magnifications. While these samples consist of only mineral, they still show a preferential orientation to their original collagen template.
Adapted from: (a) [62], (b) and (c) [64].

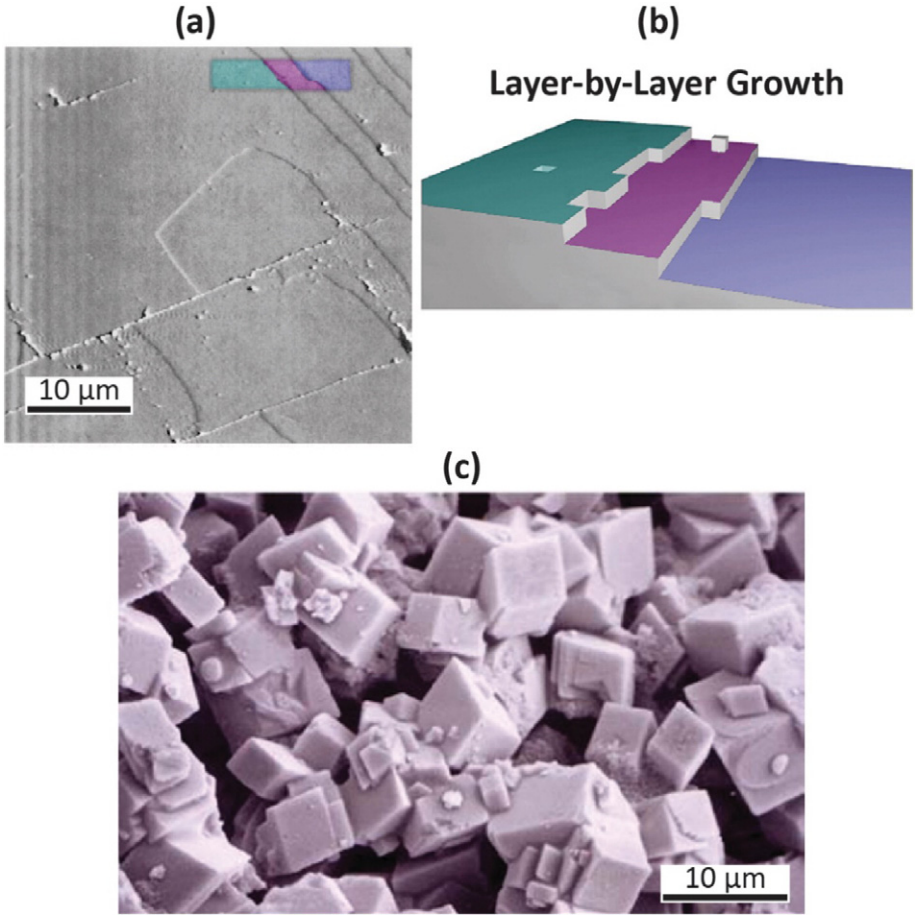

Fig. 7. Crystalline calcium carbonate structure. (a) Calcite showing the characteristic layered structure of crystallized calcium carbonate. Layers are color coordinated with (b); (b) this characteristic structure is caused by layer-by-layer growth as dictated by the diagramed Kossel model; (c) particles of calcium carbonate (calcite) showing a faceted structure. Adapted from: (a) and (b) [68], (c) [212].

the structure of the templating constituent, in these cases type I collagen fibers [62–64]. As a result, the reactivity of the templating constituent has a significant effect on the adherence and structuring of hydroxyapatite in any biological material [65].

Calcium carbonate ($CaCO_3$) is the biomineral phase in many of the highly rigid marine biological structural materials such as the nacre of abalone, conch and other marine mollusks as well as urchin spines and some crustacean exoskeletons [66–69]. Amorphous $CaCO_3$ is employed as a precursor to crystalline structures that generally take the form of aragonite (orthorhombic) or calcite (rhombohedral) depending on the growth parameters [68]. Biologically this differentiation is realized through the use of biopolymers and macromolecules as templating agents [69–71]. In structures such as mollusk nacre and sea urchin spines these crystals develop according to Kossel's model that states that growth occurs in a layer-by-layer fashion where new layers are started from island nucleation that grows in a plane until a new surface is completed (imaged in Fig. 7a and diagramed in Fig. 7b) [68], which results in faceted crystal structures (Fig. 7c). This is due to the fact that growth occurs preferentially along surfaces with steps where more than one attachment is ensured, thus lowering the total energy of each atomic attachment event. Additionally, in many marine organisms (e.g. sea urchins, corals and crabs) other minerals such as magnesium and bromine are incorporated into $CaCO_3$ crystal structures to improve the mechanical strength [72–75].

Silica (SiO_2) is most commonly expressed within the biological materials of sponges and diatoms [76–81], and is generally found in its amorphous form [76–79]. The biomineralization of SiO_2 follows different processes in different organisms. In sponges and diatoms the biomineralization of SiO_2 occurs similarly to hydroxyapatite and $CaCO_3$ by forming an essential skeleton to provide both structure and mechanical strength [4,79,82]. Given its amorphous nature, and unlike $CaCO_3$ and hydroxyapatite, there is no dominant structure of biological SiO_2 with it appearing in multiple forms (e.g. spicules, Fig. 8) in a single organism [76,83]. These silica structures are templated by biopolymers into the structural elements of many marine organisms.

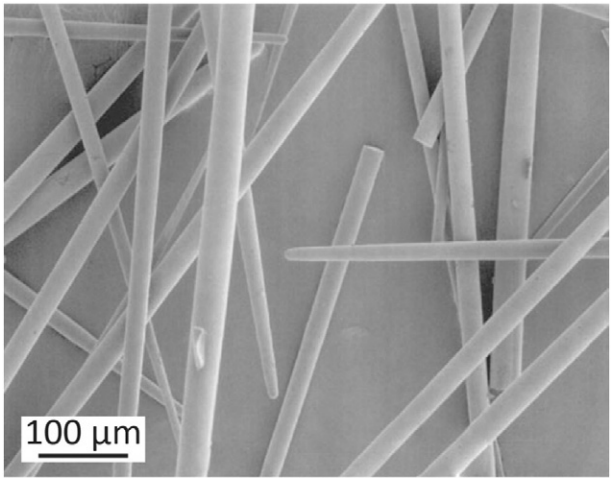

Fig. 8. Example spicule structures of amorphous silica employed in sponges and diatoms. Adapted from [82].

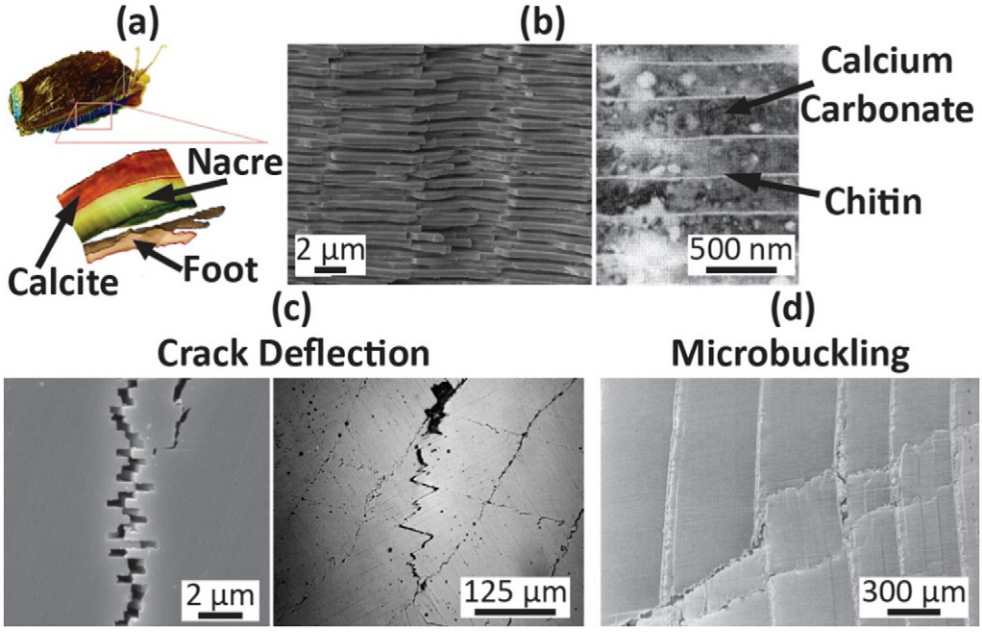

Fig. 9. Structure and toughening mechanisms of marine mollusk nacre (imaged species: *Haliotis rufescens* and *Strombus gigas*). (a) Cross-section of the abalone shell displaying the calcitic and aragonitic (nacre) layers; (b) the brick-and-mortar structure of nacre displaying calcium carbonate plates with mortar-like chitin layers; (c) crack deflection toughening mechanism that causes a more tortuous crack path; (d) microbuckling toughening mechanism in compression of the calcium carbonate plates that creates significant additional surface area. Adapted from: (a) [213], (b) [93,102], (c) [96], (d) [102].

Magnetite (Fe_3O_4) is found within a number of marine bacteria [84,85] as well as sea turtles [86,87] and some crustaceans [88]. Fe_3O_4 is rarely employed as a broad structural material in organisms, but rather within individual organs for a specific function. However, it is present as a structural material in the teeth of chitons, where it is employed in order to increase hardness [89]. Given the magnetic properties of Fe_3O_4, it is most often employed as a bio-compass allowing marine organisms such as lobsters and sea turtles to orient themselves to the earth's magnetic field and travel without other sensory cues [84,85,88,90].

Though uncommon, iron sulfide (FeS) is found within deep sea organisms: commonly bacteria, tube worms and a few gastropods, where the FeS is made available by deep sea vents [91,92]. It is often deposited on or absorbed into organisms and incorporated into their dermis to create an outer FeS shell [92].

While the biominerals described above are the most common, there are around sixty currently described minerals in biological materials. These include carbonates (e.g. vaterite), phosphates (e.g. struvite, francolite), halides (e.g. fluorite), sulfates (e.g. gypsum, barite), oxides and hydroxides (e.g. goethite, ferrihydrite) and sulfides (e.g. pyrite) [4].

3. Crushing resistant structures

3.1. Mollusk shells

Many mollusks protect themselves from predators with hard external shells composed of a brittle external calcite layer and a tough internal layer composed of aragonite, chitin and proteins, also known as nacre or mother-of-pearl (shown in Fig. 9a for the example case of abalone) [67,93–95]. These shells forfeit all flexibility in favor of high

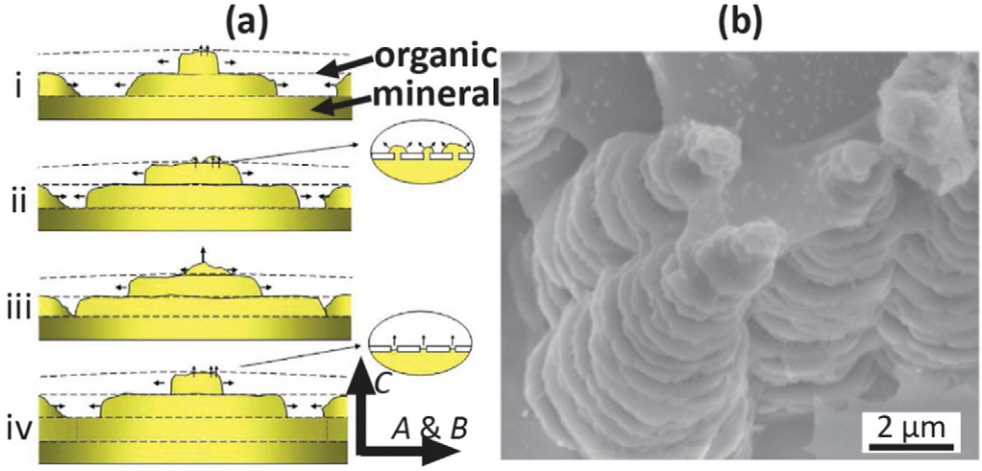

Fig. 10. Process of nacre growth in the shell of abalone (*Haliotis rufescens*). (a) Diagram of the process of nacre growth (progressing from top to bottom) where calcium carbonate mineral shelves assemble through an organic membrane. Growth occurs laterally (*A* and *B* directions) while it is retarded longitudinally (*C* direction) by deposition of a porous organic layer (dashed lines); (b) SEM image of nacre displaying the growth peaks.
Adapted from: (a) [97], (b) [99].

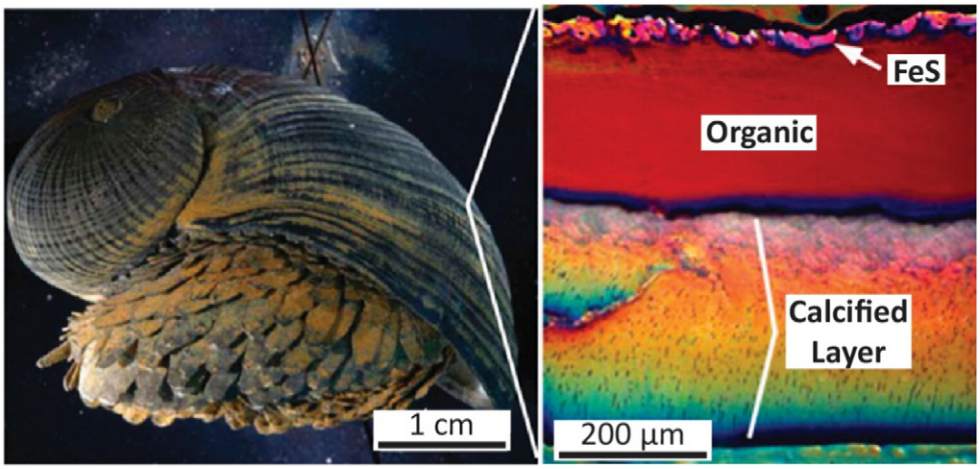

Fig. 11. Deep sea scaly-foot gastropod (*Crysomallon squamiferum*) that employs a three part shell with an iron-sulfide based outer layer (FeS), an organic intermediate layer (Organic) and an aragonite inner layer (Calcified Layer).
Adapted from [109].

strength, which is reflected in the relative proportions of rigid biomineral to ductile biopolymer found in the shells of red abalone (19:1) [96], where biomineral severely outweighs biopolymer. In spite of this, many of these shells manage to provide optimized toughness, much higher than pure calcium carbonate [7,67,93]. This is realized through the brick-and-mortar structure of nacre (Fig. 9b) [67,93,94].

In order to grow this tough microstructure, mollusks employ complex assembly techniques. In the example case of abalone, growth is mediated by an organic interlayer comprised of chitin, an organic silk and acidic proteins in such a manner that successive layers of calcium carbonate (aragonite) tablets are deposited (Fig. 10a) [95,97–100]. Naturally, the growth of aragonite crystals is highly anisotropic, with the *C* direction in the orthorhombic cell (normal to the largest surface) having a much greater velocity than either of the orthogonal *A* or *B* directions. This would lead to the formation of needle-like structures without mediation. In order to regulate the growth, the epithelial layer of the organism generates a porous chitin-based membrane and deposits it on the growth surface. The sequence shown in Fig. 10a (progressing from top to bottom) shows the deposition of one such layer and the manner by which it alters the growth. The *C*-growth direction is slowed down, while growth in directions *A* and *B* proceeds normally as the Ca^{+2} and CO_3^{-2} ions traverse the membrane. The resulting shape of the crystal is changed from a needle to a hexagonal prism. Lateral growth continues until the tablets (tiles) abut each other. In this manner, terraced cones (also called "Christmas trees") are created. Fig. 10b shows a scanning electron microscopy (SEM) image of the growth surface. This results in growth of a lamellar, brick-and-mortar structure with $CaCO_3$ tablets held together by an organic mortar and mineral bridges [95,97]. This growth has been shown to depend strongly on both nutrient availability and ambient environmental conditions [101].

At quasi-static loading rates in compression, the shells of abalone [66,97,102,103], conch [104,105] and giant clam [96] employ a variety of toughening mechanisms, realized through the brick-and-mortar structure of their nacre, including crack deflection and microbuckling of the calcium carbonate plates to induce a gradual "graceful failure." These toughening mechanisms are imaged in Fig. 9c–d. Within brittle materials, where there is limited plastic deformation to absorb energy, fracture toughness is increased by toughening mechanisms such as the ones listed above that force a crack to propagate through a long and tortuous path [106,107]. A more tortuous crack path requires that

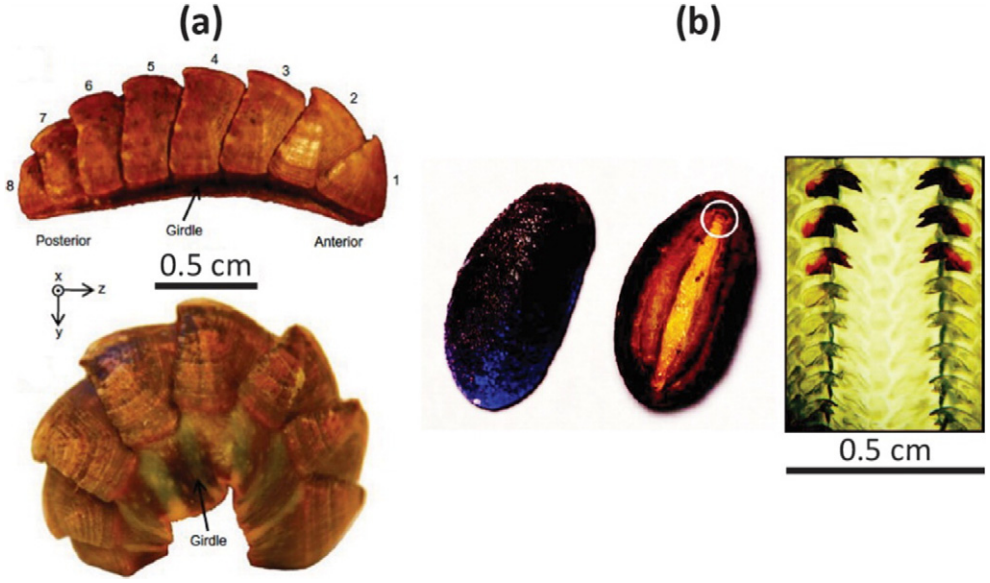

Fig. 12. (a) Lateral-view photographs of a chiton (*Tonicella marmorea*) showing the eight plates that can curl up into a defensive position; (b) another chiton species (*Cryptochiton stelleri*) displaying their characteristic mineralized teeth that are made of magnetite at the leading and trailing edges and iron-phosphate in the core.
Adapted from: (a) [113], (b) [89].

additional surface area is created to induce catastrophic failure, thereby increasing the toughness.

The brick-and-mortar structure of nacre provides a highly tortuous crack path, redirecting the crack front at angles near 90° (as shown in Fig. 9c). Of additional importance, the cases of abalone and conch both show an increase in strength of ~50% at high strain rates that are more representative of the crushing bites of predators [102,104]. Given the success of this system in the natural world, it has led to bioinspired designs of ceramics with toughness that surpasses that of their monolithic equivalents [9,108].

Beyond the toughened shells of abalone, conch and clams, there are a number of other marine mollusks that provide intriguing mechanical properties and bioinspired potential. An example is the deep sea scaly-foot gastropod *Crysomallon squamiferum* (Fig. 11), which employs an outer layer of FeS and a calcified inner layer that are separated by a relatively thick organic layer [92,109,110]. FeS is deposited on the surface of the mollusk by the deep sea vents in its natural habitat and incorporated into its structure [92,110]. These FeS deposits are referred to as "sclerites," or elements of deposited mineral that are held together by a matrix (in this case the thick organic layer) in order to form a protective coating [92].

Another intriguing marine mollusk is the chiton. Chitons have one of the more complicated shell structures of any mollusk despite being reported to be the most phylogenetically primitive. They are often referred to as "living fossils," since their appearance has not changed much in over 500 million years [111]. There are eight overlapping plates (valves) on their dorsal surface that are surrounded by a tough, leathery organic substance called a girdle, which often has mineralized scales or spicules [112]. This configuration allows the animal considerable flexibility compared to other mollusks. They can bend either upward for movement or downward to curl up into a ball for defensive purposes. Fig. 12a shows photographs of the valves and of the animal curled up. From the dorsal to ventral surfaces, six layers in mid-section valves were identified that have granular, prismatic or crossed-lamellar microstructures of aragonite crystals [113]. The interconnection between the valves was described as an actuating sandwich structure consisting of two valves separated by compliant muscles that operate to provide motion [113]. Of additional interest, the chiton *Cryptochiton stelleri* has adapted to produce extremely hard and wear-resistant teeth of Fe_3O_4 and α-chitin to scrape algae off of rocks (Fig. 12b) [89,114,115]. The teeth themselves mineralize in a four-step process: (1) forming a pure chitin scaffold tooth, (2) precipitating crystals of an intermediate and

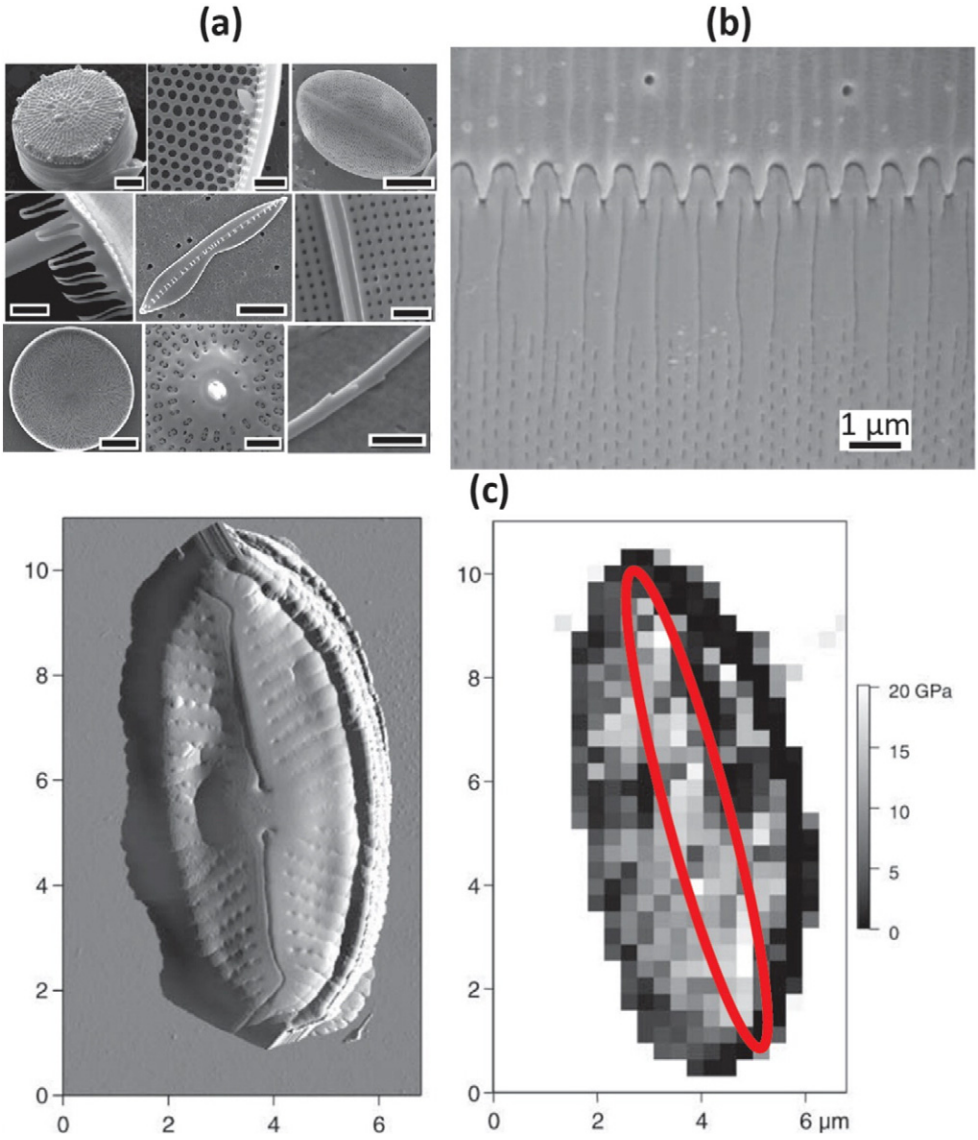

Fig. 13. (a) Diatoms displaying a wide variety in exoskeleton shape (scale bars range from 1–50 µm); (b) example of the intricate designs of diatom frustules; (c) elastic modulus results of atomic force microscopy mapping of a diatom exoskeleton showing the beam-like formation of stronger material (circled) that runs along the center of the body.
Adapted from: (a) [118], (b) [79], (c) [124].

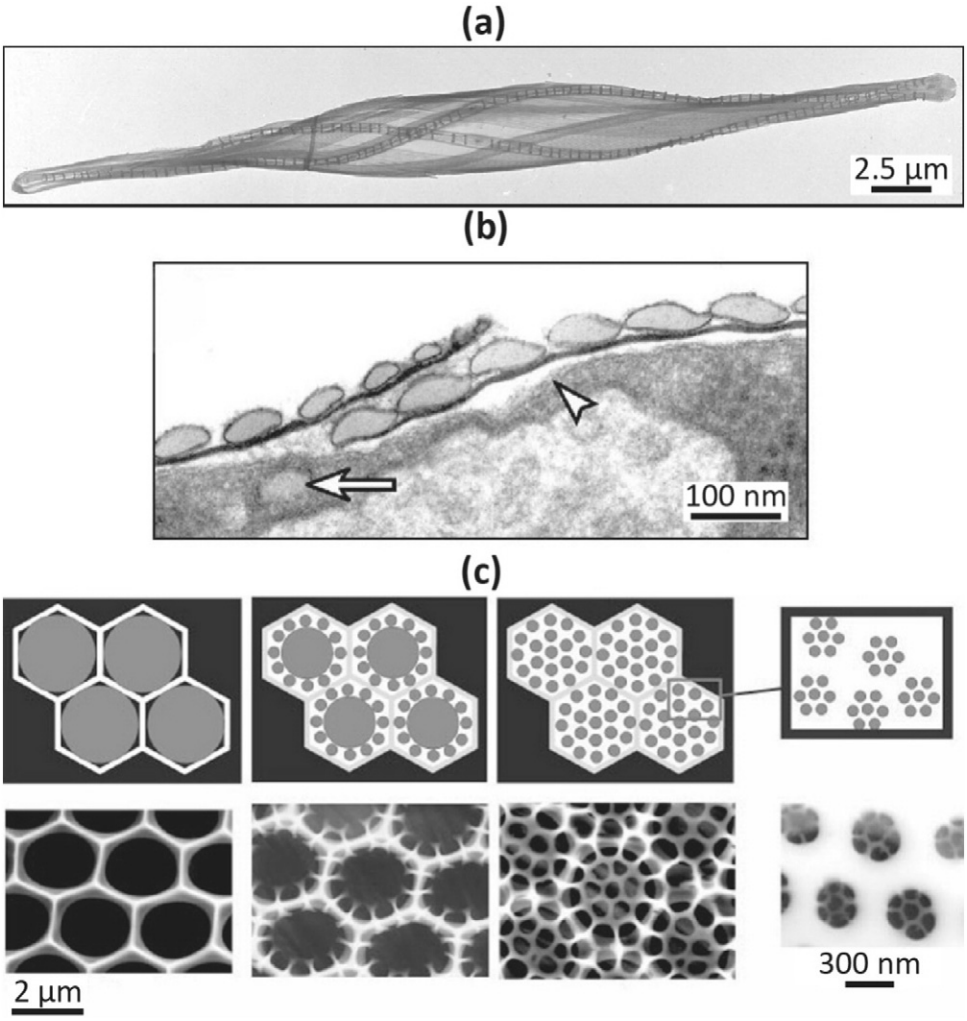

Fig. 14. (a) Diatom (*Cylindrotheca fusiformis*); (b) cross-section of the diatom showing the silica spheres (marked with arrows) being deposited on the surface of the diatom; (c) the proposed mechanism for the formation of the frustule of diatoms through continuous segregation of a silica phase (light gray) from a water phase (dark gray), steps diagramed (top) and in scanning electron imagery (bottom).
Adapted from: (a) and (b) [127], (c) [128].

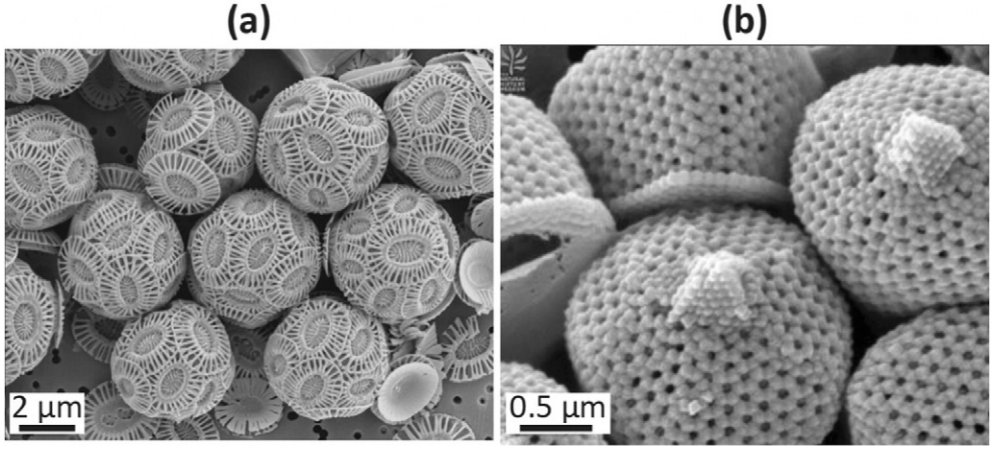

Fig. 15. Scanning electron microscopy images of coccolithophores. (a) Heterococcolith (*Emiliania huxleyi*). The unicellular organism is surrounded by calcite plates whose elements are composed of single crystals; (b) holococcolith (*Syracosphaera pulchra*). The unicellular organism is surrounded by a shell composed of small, uniform single crystals.
Adapted from [214].

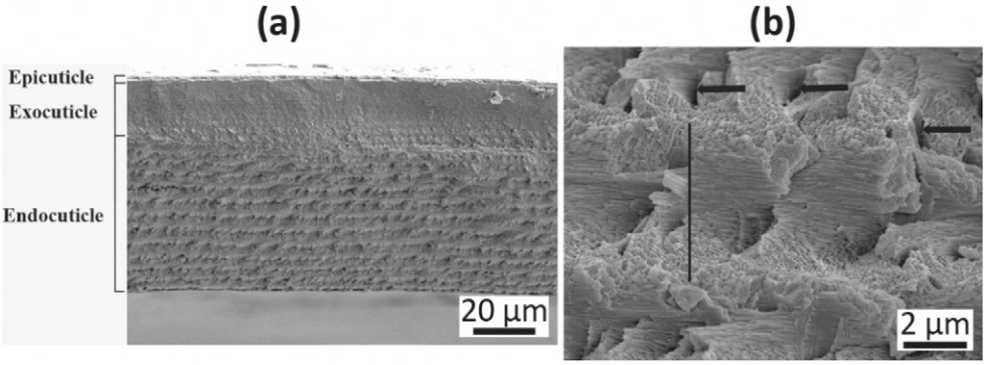

Fig. 16. Crustacean exoskeleton (*Pachygrapsus crassipes*). Images are scanning electron microscopy micrographs showing fractured cross-sections of crab cuticle: (a) the epicuticle, exocuticle and endocuticle of the cross section. There is a change in stacking density of the Bouligand layer at the interface between the exocuticle and endocuticle. The exocuticle has a greater stacking density; (b) magnified view of Bouligand layer of the endocuticle. Vertical line depicts single Bouligand layer, black arrows indicate pore canals.
Unpublished works provided by Jennifer Taylor.

metastable iron oxide (ferrihydrite), (3) transforming the ferrihydrate into Fe_3O_4 and (4) allowing for Fe_3O_4 crystal growth [89,116]. This mineralization process is driven by acidic macromolecules that pattern the chitin scaffold [116].

3.2. Diatom and coccolithophore exoskeletons

Diatoms and coccolithophores are both unicellular phytoplankton (algae). Diatoms, commonly found throughout the ocean, produce rigid external cell walls (or exoskeletons) formed from hydrated amorphous silica and range in diameters from 10–150 μm [117,118]. Despite their often microscopic size, the sheer biomass of diatoms causes them to account for 40% of the primary production of carbon [119] and the majority of biogenic silica (silica transformed from dissolved silicate into skeletal material) [120] in the oceans. While diatoms often exhibit simple geometric profiles (Fig. 13a), their surfaces (called "frustules") are adorned with complex structures (an example is shown in Fig. 13b). Both of these length scales provide structural protection. The geometric profiles provide strength against engulfing and crushing attacks from larger predators (e.g. crustacean zooplankton) while the frustule provides protection from the attacks of smaller predators (e.g. parasitoid and ingesting protists) [121]. As there is an immense number

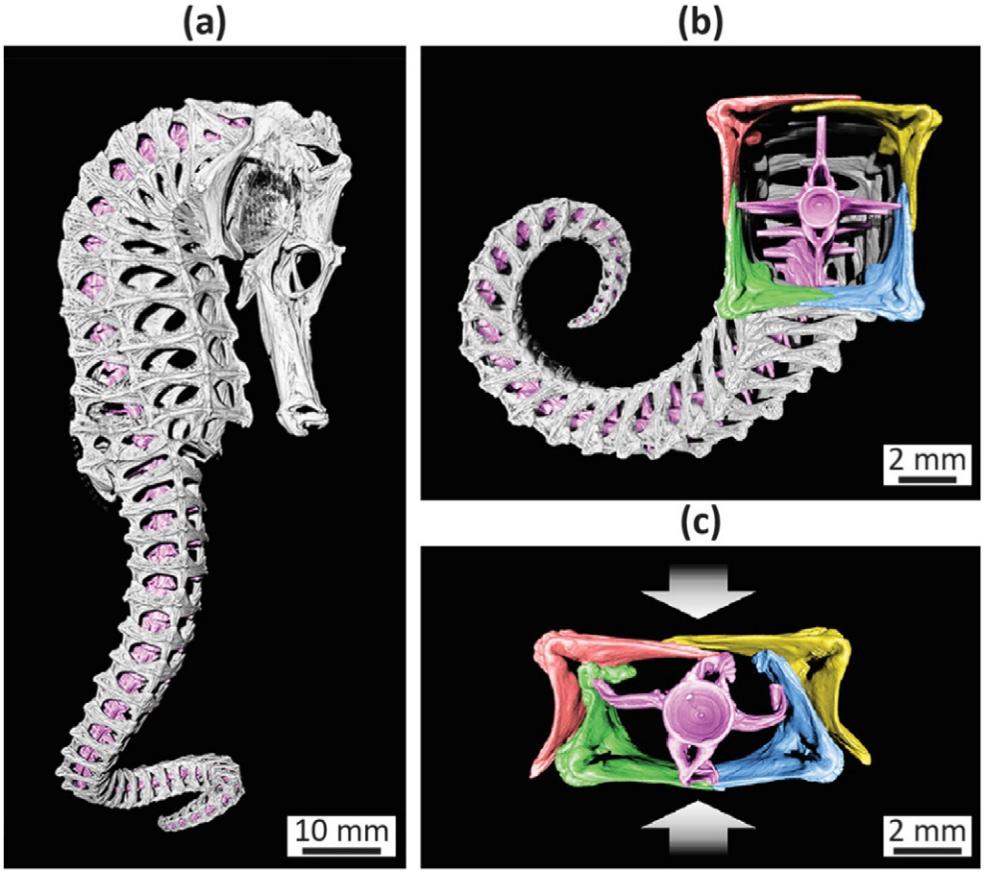

Fig. 17. (a) A micro-computed tomography image of the skeletal system of a seahorse (imaged species: *Hippocampus reidi* and *Hippocampus kuda*); (b) a micro-computed tomography image of the square seahorse tail displaying four overlapping bony segments and the central vertebra; (c) the tail cross-section subjected to compression. The skeletal armor buckles and deforms to protect the central vertebral column.
Adapted from [154].

of different profiles [122], it has been theorized that diatom species have evolved to defend against specific local predators [121]. The strength of the frustule itself varies by up to an order of magnitude along the diatom surface with the maximum strength approaching that of pure silica [123–125]. This variation has been associated with different regions of the exoskeleton's growth, with the highest strength region running along the center of the body, effectively creating a load-bearing beam of harder material (Fig. 13c) [124].

The frustules are often researched because diatoms manage to rapidly create complex structures of silica at or near room temperature [126]. This is achieved through the deposition of micro- and nano-spheres of amorphous silica by species-specific polyamines in a specialized membrane called the silica deposition vesicle (Fig. 14a–b) [126,127]. The complex structures themselves have been proposed to be the result of a continuous phase separation process where a silica phase is constantly deposited at the edges of a water phase in order to create increasingly smaller patterns (Fig. 14c) [128]. The structure of the diatom exoskeleton is controlled by the availability of the necessary nutrient: silicic acid (the naturally available silica precursor in the oceans), causing both the strength and structure to diminish when depleted [117].

Coccolithophores have a spherical shell composed of over 30 calcium carbonate plates (diameters 2–10 μm) called coccoliths (Fig. 15a). Similar to diatoms in that they possess strikingly beautiful periodic shells, they tend to be smaller, having overall diameters between 5–100 μm. The shells are thought to protect the cell from osmotic, chemical and physical shocks and from UV light [129]. There are over 100 species of coccolithophores and they are the only organisms that produce mineralized materials intracellularly [130]. There are two types: heterococcoliths, which have crystal elements with different sizes and morphologies (Fig. 15a), and the less common holococcoliths, which are composed of identical single crystal elements (Fig. 15b). In the heterococcoliths, most of the elements in the plate are single crystal rhombohedral calcite, which has a different morphology than inorganic calcite [131]. These organisms are thought to be an important indicator of ocean acidification, as they decrease the pCO_2 in the upper euphotic zone through photosynthetic fixation of CO_2 into organic molecules [132].

3.3. Crustacean exoskeletons

The crustacean exoskeleton is a multi-layered, multi-functional cuticle that affords favorable mechanical properties in a lightweight structure. The calcified cuticle is made up of chitin fibers mineralized with calcium carbonate [133], although some crustaceans employ other elements as reinforcing agents (e.g. magnesium, bromine). The cuticle is comprised of four distinct layers that differ in structure, composition, and mechanical properties. The outermost layer is the epicuticle, which is thin and mineralized [134]. As this is the outermost layer, one of its primary functions is a barrier to the external environment. Beneath the epicuticle lies the procuticle, subdivided into the exocuticle and endocuticle, which serve as the load bearing layers. Both the exocuticle and endocuticle are composed of a chitin–protein matrix embedded with mineral. The epicuticle, exocuticle and endocuticle are displayed in Fig. 16a. Chitin and protein bundles are arranged in horizontal planes, or lamellae, that are stacked into a helicoid, or Bouligand, structure (highlighted in Fig. 16b) [135]. A series of pore canals traverse the lamellae of both the exocuticle and endocuticle, creating a honeycomb-like structure that contributes to the strong, lightweight design [136]. Generally, the endocuticle is the thickest and most variable layer. The fourth, innermost membranous layer is a non-mineralized matrix, which is present in only some crustaceans and is not thought to contribute to the cuticle mechanical properties.

Although the load bearing layers have the same architecture, they differ in stacking density and crystallinity, affording a gradient of mechanical properties. Typically, the exocuticle lamellae are denser than those of the endocuticle [133,137]. The crystallinity of the exocuticle not only differs from the endocuticle, but it also exhibits a gradient within it; amorphous calcium carbonate occurs in the proximal end, near the interface with the endocuticle, and transitions to calcite at the distal end [138,139]. In contrast, the endocuticle contains magnesium calcite and amorphous calcium carbonate [139]. These differences result in the exocuticle being both harder and stiffer than the endocuticle [133,137,140–142]. As the exocuticle increases in hardness toward the interface with the endocuticle, there is an

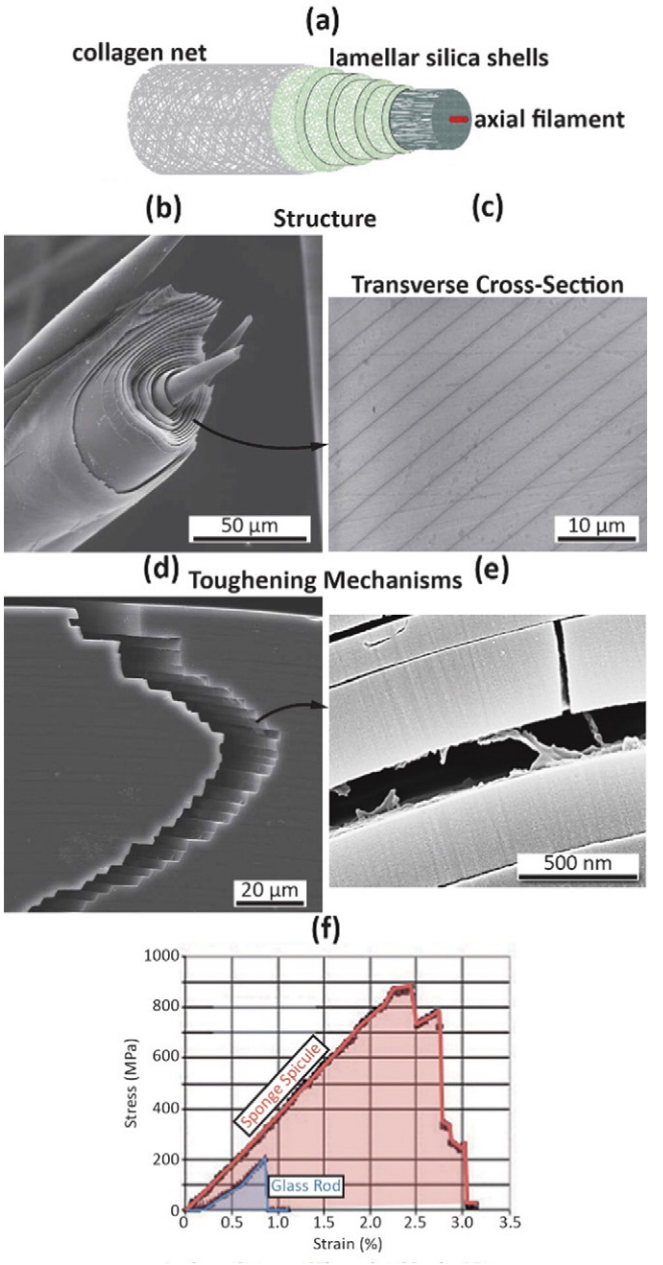

Fig. 18. (a) Diagram of the structure of a sea sponge (imaged species: *Euplectella aspergillum* and *Monorhaphis chuni*) spicule showing the axial filament (silicatein), the surrounding silica shells and exterior collagen net; (b) etched microstructure of a sea sponge spicule showing the concentric silica rings (shells); (c) transverse cross-section of a silica spicule showing the concentric tree-like rings; (d) fracture of a spicule showing significant deflection of a crack passing through the silica rings; (e) magnified fracture displaying the thin layer of silicatein (protein) between the silica rings; (f) mechanical data displaying the significant increase in toughness of a sponge spicule over a sample of similar geometry made up of the spicule's main constituent, silica glass.
Adapted from: (a) [156], (b)–(d) [161], (e) [158] (f) [215].

abrupt change in both hardness and stiffness of more than an order of magnitude between these two layers [137].

Despite the cuticle being brittle and prone to delamination [133,143,144], the Bouligand structure of the procuticle layers affords some toughness by crack deflection and bridging, which force cracks to propagate in a tortuous, stepwise fashion [142]. The ductile pore canal tubules are also thought to enhance toughness, as necking is observed during tensile testing normal to the cuticle surface [133].

Crustaceans exhibit variation in cuticle mineralization and structure (e.g. layer thickness, stacking density) across species and across functional regions within an individual. For example, appendage joints contain non-calcified arthrodial membranes that must remain soft and flexible to permit rotation [145]. There are also great differences between the cuticle of the carapace, which protects internal organs and resists compression, the walking legs, which primarily resist muscle contraction forces, and the claws, which function as weapons and prey capture devices. In crab claws, for example, the exocuticle is 3–4 times harder than the walking leg exocuticle, and this is primarily due to its greater mineral content [133]. The effectiveness of claws in securing prey depends not only on their hardness, but also on their resistance to cracking and abrasion. In some crabs, such as stone crabs, the claw tips are darkly pigmented and even harder and tougher than non-pigmented areas, possibly due to the increased cross-linking associated with tanning and reduced porosity [146]. Other crabs, such as shore crabs, enhance their claws by adding bromine rich tips that can afford an order of magnitude increase in fracture resistance compared to calcified tips [74,75].

The intricacy and variability of the crustacean cuticle is even more impressive considering that, unlike mollusk shells that form by accretion, crustaceans repeatedly shed and secrete a whole new cuticle during the process of molting. The secretion of matrix to form the cuticle layers and the subsequent deposition of mineral occur rapidly, over the course of days, and as frequently as once per week in small juveniles. Cuticle formation is a conserved and intricate process, but can be affected by environmental conditions such as ocean carbon chemistry.

3.4. Seahorse skeleton

Seahorses (*Hippocampus*) have plated skeletons that cover their bodies and prehensile tails (Fig. 17a). Unlike most fish, seahorses swim upright, utilizing their dorsal fin for propulsion and two pectoral fins for maneuverability, resulting in slow swimming velocities [147–149]. Thus, they use their prehensile tails for stability, gripping and holding onto objects such as sea grasses, mangrove roots, and coral reefs [147]. The tail skeleton is composed of several articulating segments arranged into cross-sectional squares, each composed of four bony plates that surround a central vertebra (Fig. 17b) [147–154]. These plates are connected by overlapping joints that allow them sufficient flexibility for grasping as well as added strength for armored protection [154]. In grasping, the square structure of the tail provides more surface contact and a mechanism for maintaining organization of the articulating plates [154]. When the tail (of a deceased seahorse) is crushed, it can be compressed up to nearly 50% of its original width before fracture of the vertebral column (Fig. 17c) [150]. This unique energy absorption mechanism provides seahorses protection against predators, many of whom attack by crushing (e.g. claws of crabs, beaks of sea turtles and birds) [155].

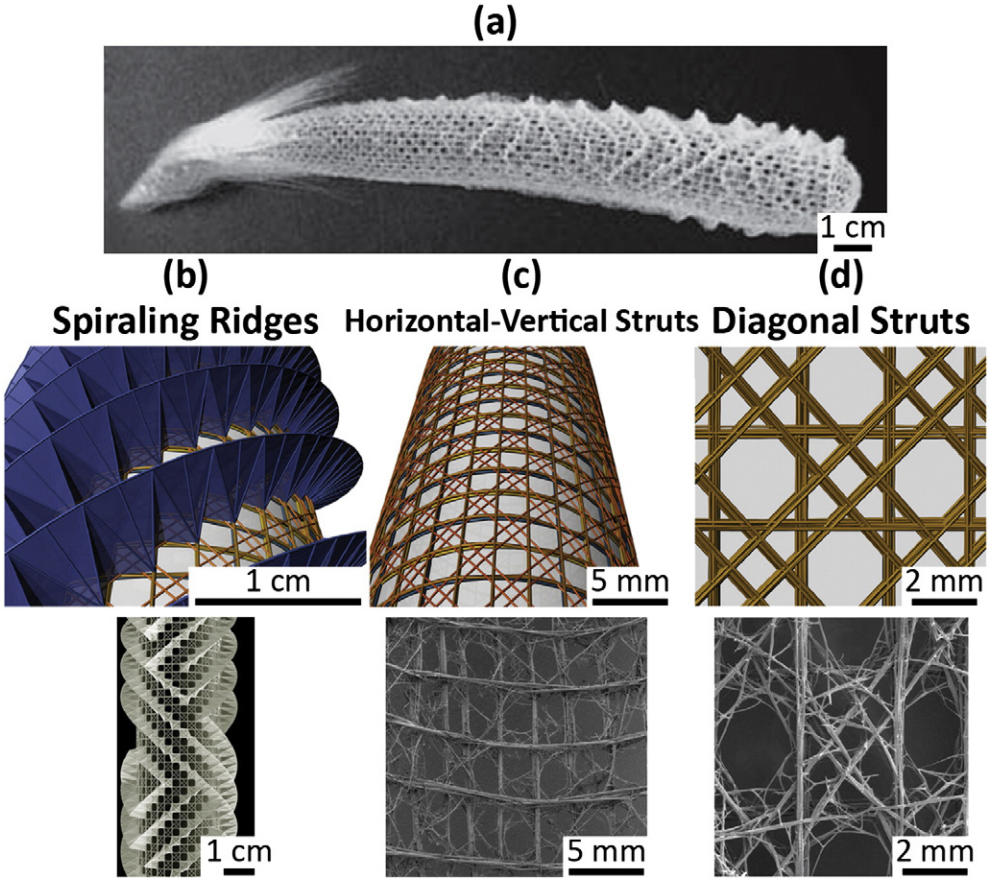

Fig. 19. (a) Hierarchical skeleton macrostructure of the Venus' flower basket sponge (*Euplectella aspergillum*). Examples of the complex structure of struts that *Euplectella aspergillum* employs with diagrams, optical microscopy and scanning electron microscopy images: (b) exterior spiraling ridges; (c) horizontal and vertical struts where the horizontal struts are predominately on the interior of the lattice and the vertical struts are predominately on the exterior of the lattice; (d) diagonal struts.
Adapted from: (a) [158], (b)–(d) [157].

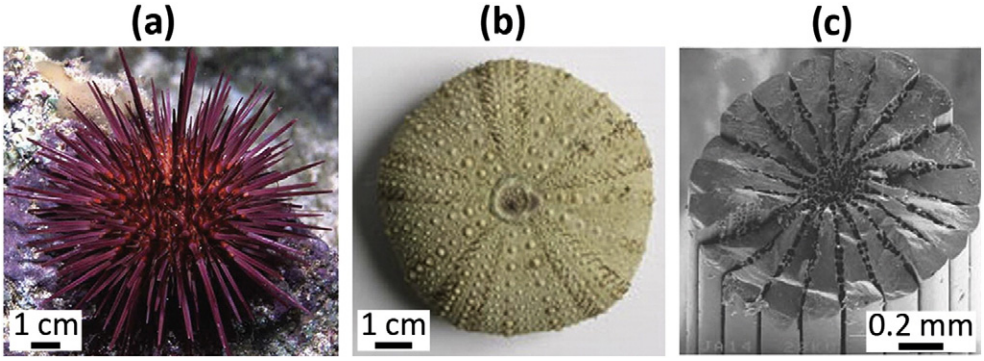

Fig. 20. (a) Photographs of a common sea urchin (*Paracentrotus lividus*); (b) the sea urchin test; (c) scanning electron microscope image of the fracture surface of a spine. Adapted from: (a) www.puntacampanella.org, (b) www.aeonwebtechnology.com, (c) [216].

4. Flexure resistant structures

4.1. Sea sponge spicules

Sea sponges produce a rigid skeleton to provide both structure and protection from predators. This skeleton is made up of needle-like spicules of amorphous silica, templated by axial collagen fibers [10,11,82,156–158] that are encased in a collagen net [10,156]. The structure is diagramed in Fig. 18a. Of particular interest, silica is not necessary for growth of the sponge as it has been shown that, when deprived of silica, the silicatein (protein) axial filaments will continue to grow [159]. The structure (Fig. 18b–c) consists of concentric rings (similar to tree rings), which surround the axial filament. While not to the extent found in mollusk shells, sea sponge skeletons are highly mineralized (3:1 biomineral to biopolymer [82]). These rings are held together with a "mortar" of silicatein [2,82,157,158,160]. The sea sponge employs the toughening mechanism of crack deflection (Fig. 18d–e) to create an elongated and more tortuous crack path [161], thus increasing the fracture toughness significantly over that of its pure constituent, silica glass (Fig. 18f) [161].

While the microstructural toughening mechanisms of sea sponges provide for a strong biological structural material, certain species employ additional hierarchical mechanisms as well. *Euplectella aspergillum* employs a complex macrostructure skeleton in order to provide high bending and flexural strength while minimizing material volume (Fig. 19a) [157,158]. It utilizes a lattice of longitudinal, transverse and diagonal struts (each comprised of a bundle of spicules) in order to resist forces in a wide range of directions (Fig. 19b–d). Around the exterior, spiraling ridges are aligned at an angle of ~45° in order to resist the maximum structural torsion and bending forces (Fig. 19b). Reinforcements such as these (set at 45°) have been shown to best resist torsional forces in composite structures [162].

4.2. Sea urchin spines

Sea urchins belong to the phylum Echinodermata, which also include sea cucumbers, starfish and sand dollars. Urchins are characterized by having five-fold symmetry, a collagenous dermis overlying an endoskeleton (test) formed by fusion of calcite ossicles (plates) and spines that radiate from the test. An example of an urchin (*Paracentrotus lividus*) and its test are shown in Fig. 20a–b.

Urchins are highly diverse, ranging throughout every marine environment from polar to tropical temperatures and down to depths of 5000 m. Most of their spines are long and pointed, since they function as protection from predators. Spines can range up to 30 cm in length and up to 1 cm in diameter [163]. Fig. 20c shows a spine fracture surface imaged by SEM from *P. lividus*, illustrating 20 plates that radiate from a central core. The spines are porous crystals of a highly Mg-substituted calcite, $Mg_xCa_{1-x}CO_3$ ($0.02 \le x \le 0.15$). Substitution of Mg into the calcite structure results in a harder material. Fig. 21 shows SEM micrographs of a *Heterocentrotus mammillatus* spine, revealing a radial sequence of porous and dense layers that are attributed to growth rings. There is a gradient in porosity, with porosity increasing substantially from ~10% on the surface and in the growth rings to ~60% in the medullary core. These spines are a model for biologically controlled crystal growth and consist of a mesocrystal [164,165]. Originally

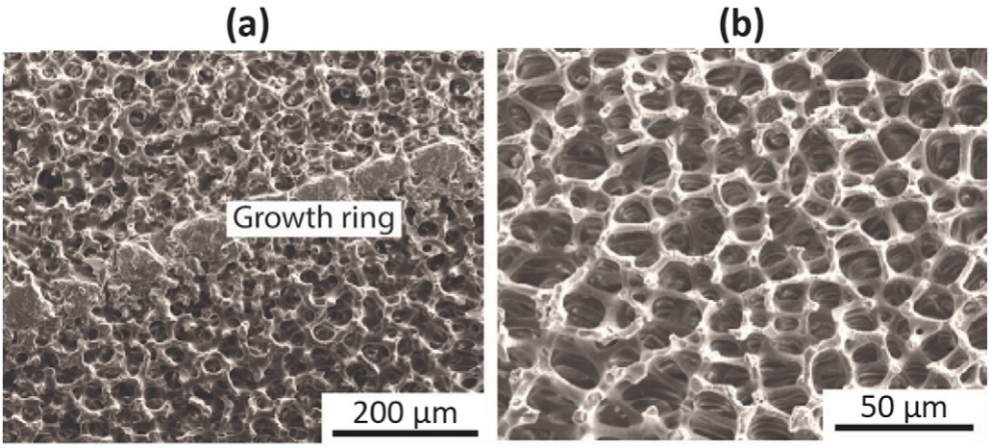

Fig. 21. Scanning electron micrographs at varying magnifications of a cross-section from a spine of the sea urchin, *Heterocentrotus mammillatus*, displaying the porous bulk and dense growth rings. The growth rings likely result from former exoskeleton surfaces.
Adapted from [163].

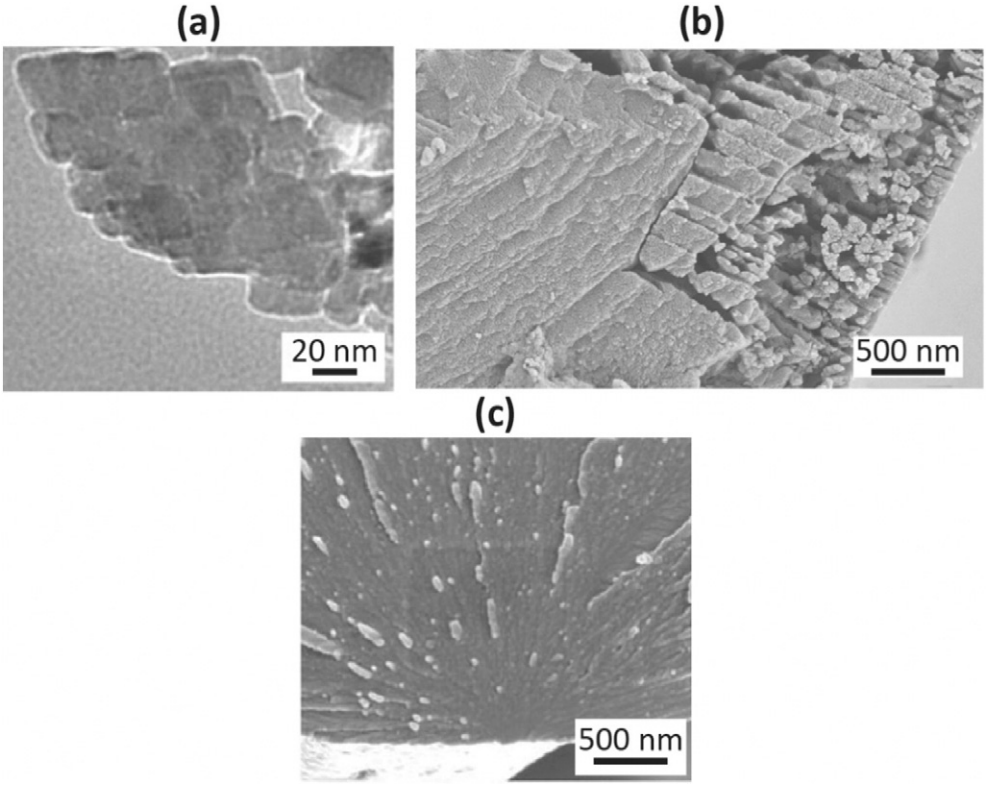

Fig. 22. Structural features of sea urchin (imaged species: *Echinometra mathaei*, *Anthocidaris crassispina* and *Authoeidaris erassispina*) spines. (a) Transmission electron microscopy image of the nanocrystals from spines; (b) etched transmission electron microscopy image of the mesocrystal structure of spines; (c) scanning electron microscopy image of the spine fracture surface displaying a similar structure to glass fracture surfaces.
Adapted from: (a) and (c) [165], (b) [164].

thought to be a single crystal [166,167], it has recently been shown that the structure consists of periodic and uniform nanocrystals, 30–50 nm in diameter, with parallel crystallographic alignment (Fig. 22a–b) [68, 163–165]. These nanocrystals are held together with layers of amino acids (mainly aspartic and glutamic acid) with a thickness of several hundred nanometers [165–167]. This results in a structure that fractures in a manner similar to glass (Fig. 22c) but presents the diffraction pattern of a single crystal [164].

Mechanically, the spines have been shown to preferentially fail at the proximal end when tested in a bending mode, which was found to be associated with the relatively higher concentration of magnesium at the base of the spine [168]. This, coupled with the fact that sea urchins are capable of repairing and regenerating spines that have been damaged or completely severed [169,170], suggests that the spines themselves are designed to fracture when stressed, potentially remaining within a predator to deter further attack. Fig. 23 shows a sketch of the cross-section, an X-ray computer tomography micrograph along the length of a *H. mammillatus* spine and compressive force–displacement data [163]. The compressive force–displacement curve displays a graceful failure instead of the catastrophic failure typified by monolithic ceramics. The force–displacement curve resembles that of a classical cellular solid, as described by Gibson and Ashby [171]. The peak stress is related to the strength of the dense outer sheath, whereas the subsequent plateau region relates to the failure of the highly porous region, dependent on the density and other elastic properties of the solid material. This value is similar to the bending strength of spines of another species (*Heterocentrotus trigonarius*), which contain 80 nm protein inclusions [172]. Furthermore, it was pointed out that the strength to weight ratio of the spines is greater than that of mollusk shells and calcareous rocks, indicating that the animals use calcite with high efficiency [173].

Though not a protective structure, the teeth of the sea urchin have garnered a significant amount of interest for their complex self-sharpening and self-assembly mechanisms. These teeth, despite being composed primarily of calcite, are able to grind through rocks of a similar composition [174–176]. This is achieved by highly aligned and continuous growth of Mg-reinforced calcite that results in self-sharpening grinding tips [174,176]. The Mg concentration increases toward the distal end of the teeth resulting in strengthened tips that can grind away calcite rocks.

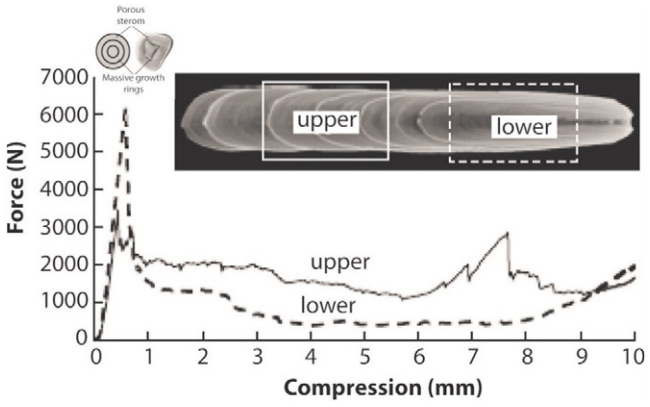

Fig. 23. Force–deflection curve for a spine from the slate pencil urchin (*Heterocentrotus mammillatus*) showing a graceful failure mode. Top left image is a diagram showing the growth rings and porous interior (stereom). Top right image is an X-ray computed tomography image showing higher (light grey) and lower (dark grey) density regions.
Adapted from [163].

Fig. 24. Micro-computed tomography image of a porcupine fish (*Diodon holocanthus*) displaying the long spines embedded within the skin of the fish.
Unpublished works provided by Frances Su (UCSD).

4.3. Porcupine fish spines

Within the order Tetraodontiformes [177], the spines of Diodontidae (porcupine fish) (Fig. 24) have developed to provide an active form of defense. These long spines are embedded within the skin of the fish and can, in many species, become erect as the fish inflates [178] and similar to the spines of the sea urchin, must be capable of resisting bending and flexure in order to provide effective defense. These spines are controlled by arrays of collagen fibers that wrap around the base [178]. In spite of this inventive protective mechanism, there is a current lack of knowledge concerning the mechanical and material properties of these spines.

5. Piercing resistant structures

5.1. Overlapping fish scales

Fish scales provide protection from a variety of predators by integrating highly ordered type I collagen fibers with hydroxyapatite biomineral [13,179,180]. Scales are composites that are composed of multiple layers. These generally include mineralized collagen and enamel-like (or bony) layers (example shown in Fig. 25a) [13, 180–182]. When a collagen layer is formed, it often has a Bouligand-like structure in order to provide increased toughness and strength in many directions [44,183]. Scales are most commonly arranged in overlapping sheets that allow for smooth motion of the body for locomotion while ensuring full coverage for protection from predators [13,180]. This overlapping pattern minimizes drag to ease swimming by regulating wave propagation about the body [184–186]. While scales can vary greatly in size, shape and arrangement from species to species, they have been classified into three relevant general groups: placoid, elasmoid (with two sub-groups: cycloid and ctenoid) and cosmoid [13, 180]. A fourth group, ganoid scales, is rare and only reported in predominantly freshwater fish such as gars [187] and bichirs [181] and, as a

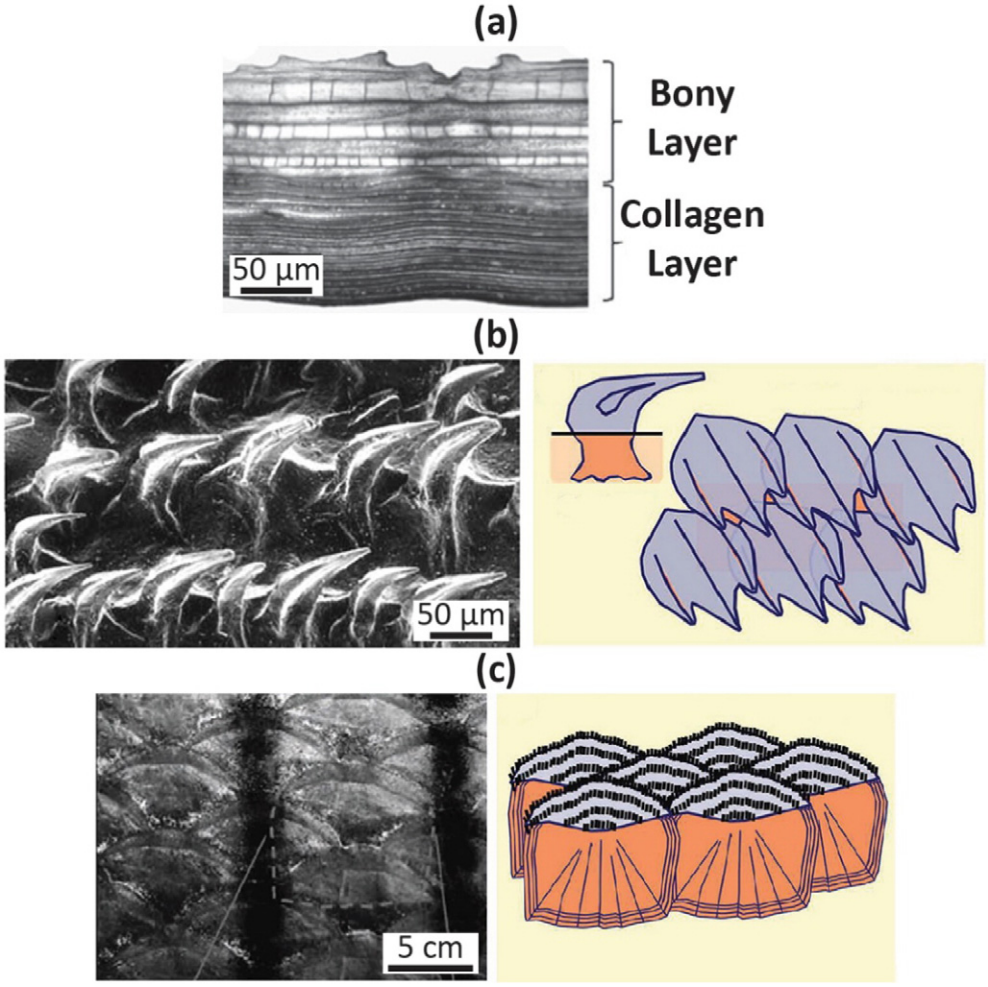

Fig. 25. Marine fish scales. (a) Cross-section of an elasmoid scale (from a striped sea bass, *Morone saxatilis*) displaying bone and collagen layers. Major marine fish scale groups: (b) scanning electron microscopy image and diagram of a placoid scale (from a catshark, *Scyliorhinus canicula*); (c) image and diagram of an elasmoid scale (ctenoid, from a striped sea bass).
Adapted from: (a) [180], (b) [13,188], (c) [13].

result, will not be discussed here. Finally, a fifth group, scutes, will be discussed later.

Placoid scales (Fig. 25b) are found on many cartilaginous fish, including sharks and rays. In shark species, they are specified as odontodes, where they display a "tooth-like" appearance [188]. They consist of an outer layer with large vascular spaces and a lamellar inner layer [189]. As these are cartilaginous fish and are without bone, the same applies to their scales. Placoid scales are specifically designed to have a surface structure that generates small-scale vorticities in water, thereby decreasing drag.

Elasmoid scales can be subdivided into cycloid and ctenoid scales (ctenoid scale imaged in Fig. 25c). They are found in teleosts, a major group of marine and freshwater fish that includes more than 26,000 species within 40 orders and 448 families; the majority of living fishes are members of this group, including the striped sea bass (*Morone saxatilis*) [180,190,191] and sea bream (*Pagrus major*) [64]. Cycloid scales, found mainly in soft fin ray fish, such as salmon, carp and eels, have a smooth margin. In contrast, ctenoid scales, found mostly in spiny fin ray fish, such as perch, grunion and swordfish, have a comb-like scale with teeth or serrations on the margin. Through the cross-section, the ctenoid scales of the striped sea bass have a bony outer layer and a collagen inner layer with the same thickness [180]. The collagen layer is formed from 4–5 μm thick collagen lamellae, which are oriented in a Bouligand arrangement that varies from species to species [180]. These collagen fibrils are mineralized at the scale's smallest length-scale, forming a staggered array with nanoplatelets of hydroxyapatite between the heads and tails of the molecules.

Latimeria (coelacanth) (Fig. 26a) are one of very few extant species, others include certain *Neoceratodus* (lungfish), known to exhibit cosmoid scales (Fig. 26b). The first live coelacanth, long considered extinct, was caught on the east coast of South Africa in 1938. The scales consist of isopedine (dense lamellar bone), spongy bone and cosmine (similar to dentin) layers [189,192–194]. Given their scarcity, the exact structure of cosmoid scales is of debate. Smith et al. [192] found that the isopedine layer consists of densely packed collagen fibers and only the most superficial portion of the scale is mineralized, while other investigators [193–195] contrarily held the opinion that the entire scale was mineralized. New research has been able to clarify this discrepancy and has shown that the scales consist of a highly mineralized surface and less mineralized base [196]. Similar to elasmoid scales, this collagen base is formed from lamellae of collagen fibers, however, these cosmoid scales also exhibit struts that connect adjacent lamellae and provide additional rigidity (Fig. 26c) [196].

Fish scales are generally designed to defend against the bites of piscivorous predators. Mechanically, this can be translated to piercing forces applied by sharp and/or jagged objects with a small surface area (i.e. teeth) [25,197,198]. This requires a composite with a surface strong enough and hard enough to withstand the high stresses and piercing nature of teeth without fracture and a base with enough toughness and ductility to absorb the compressive force of jaws and distribute it over a broader area. All fish scales achieve both of these goals with a heavily mineralized outer layer made of ganoid or hydroxyapatite-based coatings and a tough base usually made of bone or collagen fibers. This has been experimentally shown on the scales of the striped sea bass [191] where the hardness decreases through the thickness of the scale toward the proximal surface [181,198]. Of note, this collagen base has been shown to be amongst the toughest biological materials known [199]. In addition to the mechanical properties of the fish scale layers, there are specific design qualities that dictate the ability of scales to provide protection while still maintaining mobility and minimizing weight. These include the amount of overlap or imbrication, the ratio of the scale length to thickness and the ratio of the scale length to the overall fish length.

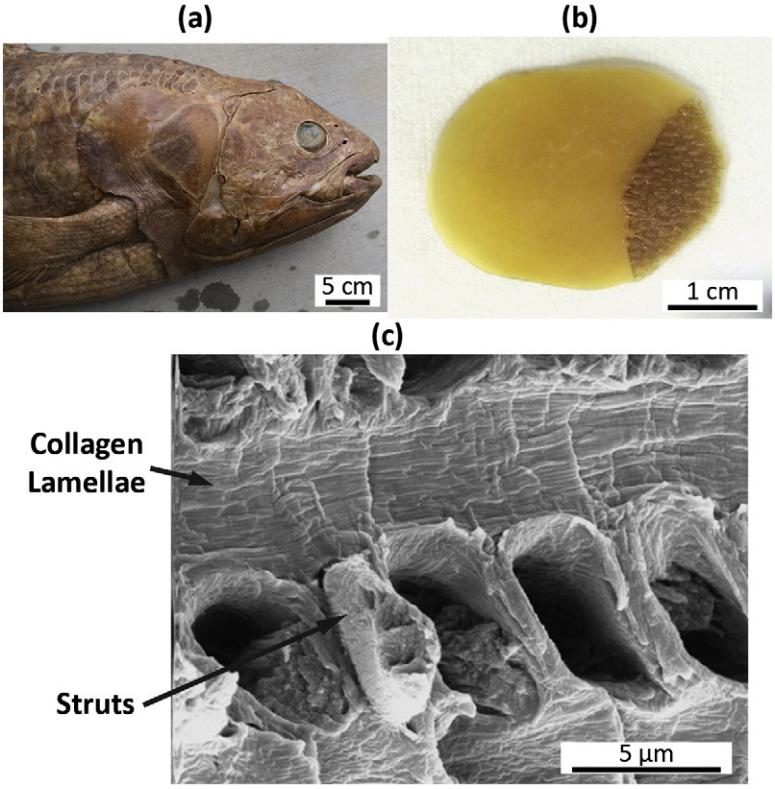

Fig. 26. Cosmoid scales from a coelacanth (*Latimeria chalumnae*). (a) Coelacanth; (b) cosmoid scale; (c) micrograph of the cross-section of the cosmoid scale displaying the distinctive struts that bridge between collagen lamellae and provide additional strength.
(a) is unpublished work provided by Haochan Quan (UCSD), (b) and (c) are adapted from [196].

5.2. Marine scutes and skeletal armors

While most fish scales are overlapping, the examples of both fish scutes and marine skeletal armors provide alternative modes of protection. Similar to fish scales, both are composites that consist of hydroxyapatite and collagen. While still providing effective protection against predators, these armors do so in distinct ways.

Sea turtles employ plated skeletal armor, which is formed from individual osteoderms, the bone-like reptilian counterpart to scales [13,200]. These exhibit a cellular sandwich structure consisting of a porous interior and dense exterior allowing for weight savings while maintaining stiffness. The leatherback sea turtle (Fig. 27a, *Dermochelys coriacea*) is of particular interest as it is capable of diving to depths in excess of 1200 m [201]. This is made possible by sutured interfaces between the osteoderms of its shell (Fig. 27b–c), allowing it some flexibility (up to ~15° of rotation) in order to accommodate the severe hydrostatic pressures of the turtle's deep ocean environment, which can reach as high as ~10 MPa (at 1200 m of depth) [13,200]. Specifically, the sutured interface employs a gap between the osteoderms (Fig. 27d) along with an array of tri-dimensional suture teeth (Fig. 27e) that enable this flexibility.

The scutes of boxfish (Ostraciidae) provide a very different mechanism for protection than fish with overlapping scales. These scutes are composed of a rigid mineral surface (hydroxyapatite-based) and a

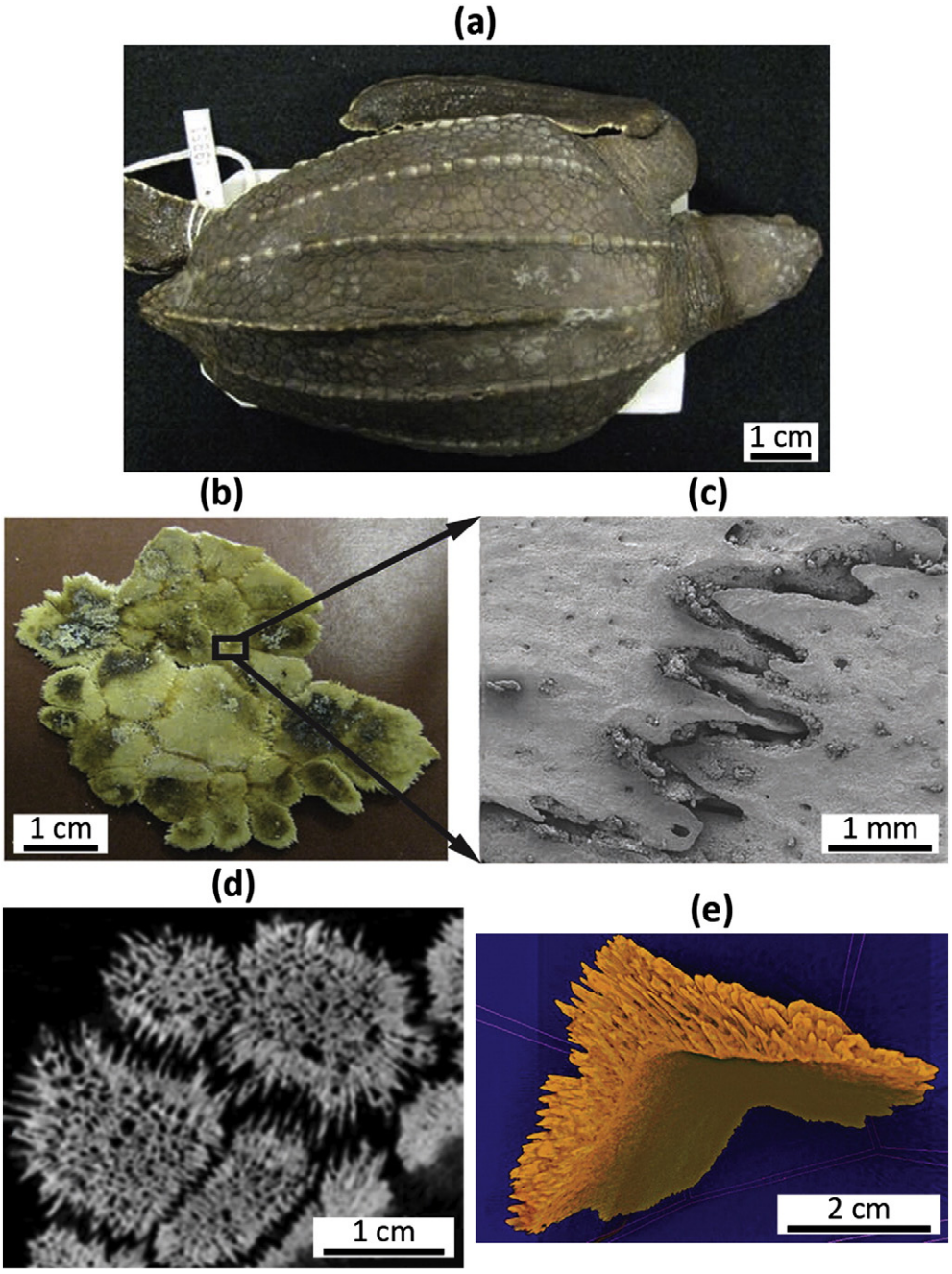

Fig. 27. Leatherback sea turtle (*Dermochelys coriacea*). (a) Leatherback sea turtle; (b) a section of carapace displaying osteoderms connected by sutured interfaces; (c) scanning electron microscopy micrograph of the sutured interface of two osteoderms; (d) micro-computed tomography image displaying a highly random porous morphology and gap between osteoderms that enable flexing; (e) micro-computed tomography image of a single osteoderm showing a 3D arrangement of sutures.
Adapted from: (a)–(c) [13], (d) and (e) [200].

compliant collagen base (type I collagen) (Fig. 28a) [12,202]. While these constituents are similar to other fish scales, the way that they are implemented is quite different, with non-overlapping scutes that connect with sutured interfaces. The ratio of biomineral to biopolymer in the scutes is 1:2 [12] which is in stark contrast to many other dermal armors such as the seahorse (~2:1) [150] and alligator (~2:1) [203]. This suggests an armor based primarily in collagen as opposed to more common mineral-based armor. Of additional interest, when mechanically tested, the mineral surface remains intact while the collagen base deforms significantly (Fig. 28b–c) [12]. While this likely lowers the overall strength, it ensures that failure occurs in a predictable and controlled manner.

6. Impact resistant structures

6.1. Mantis shrimp dactyl club

The mandible of the mantis shrimp (highlighted in Fig. 29a) is perhaps the most remarkable adaptation of the crustacean cuticle. It must resist tremendous impact forces as they rapidly unfurl to strike hard-shelled prey. The impacting surface of the smashing mantis shrimp species, the dactyl club, changes in structure from an inner bulk area of chitin fibers to an outer, heavily calcified surface, with the highest degree of crystallinity at the impact surface (Fig. 29b) [204,205]. The bulk area primarily contains amorphous calcium carbonate that transitions to amorphous calcium phosphate [205,206] and then ultimately a hyper-mineralized fluorapatite with calcium phosphate at the surface [204]. These changes in crystallinity and mineral result in increasing stiffness and hardness toward the impact surface, with hardness six times greater in the impact region [204–206]. Similar to other regions of cuticle, the impact region is toughened with chitin that absorbs energy and limits crack propagation. In the dactyl club, cracks typically nucleate in the bulk region and are deflected in the impact region due to a modulus mismatch, which contains cracks mostly within the bulk region [205]. In this region, cracks propagate in a helicoidal pattern, creating a larger crack surface area, and are stopped quickly when traversing the helicoid trajectory by an oscillation in stiffness [205]. In addition, this structure has been shown to effectively disperse the stress pulse waves generated during impact [207]. Combining a hard outer layer with an inner, energy dispersive matrix is reminiscent of human-made impact resistant armor.

7. Bioinspired materials potential

The study of protective marine biological materials is leading to significant bioinspired materials and designs. These allow for the lessons learned from marine biological materials to affect and improve everyday life. Though not an extensive list, we provide a few examples here as an introduction to the materials and research provided by bioinspiration.

- Crush resistant, high toughness ceramics based upon the tough and highly mineralized shells of abalone [9,108]: the nacre-inspired brick-and-mortar structure of these ceramics are fabricated through an ice templating process called “freeze casting” [57] followed by compression and infiltration with a second phase. They can be infiltrated with polymers or metals to form composites whose toughness is significantly greater than that of their base constituents.
- Flexure resistant fiber optics based on strong and tough silica spicules of sponges [10,11]: the structure of the spicules is comprised of three sections: a core with a high refractive index, a low refractive index cylindrical tube and an outer portion with a progressively increasing refractive index [10]. These properties allow for effective light transmission. More importantly, the layered structure provides enhanced toughness.

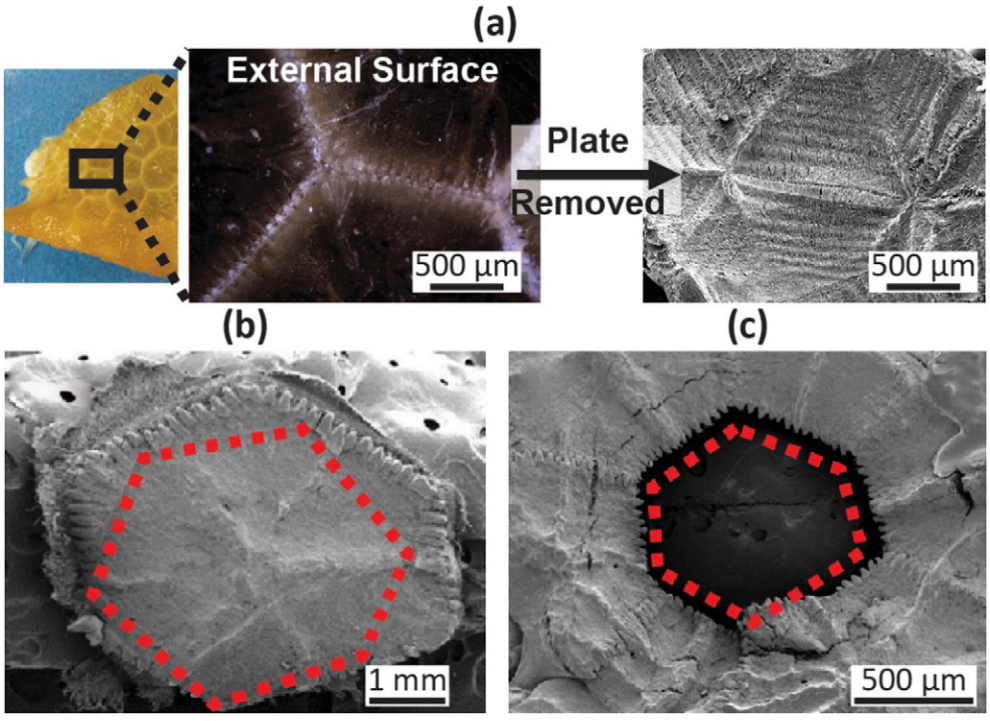

Fig. 28. (a) Structure of the lateral scutes of the boxfish (*Lactoria cornuta*), the external surface is mineralized and rigid, but if removed, a base of aligned collagen fibers is revealed; (b) fracture of a scute tested in a punching mode by a hexagonal punch (highlighted); (c) fracture of the surrounding scutes. In both cases, the facture occurs primarily within the collagen base while the mineral remains relatively intact.
Adapted from [12].

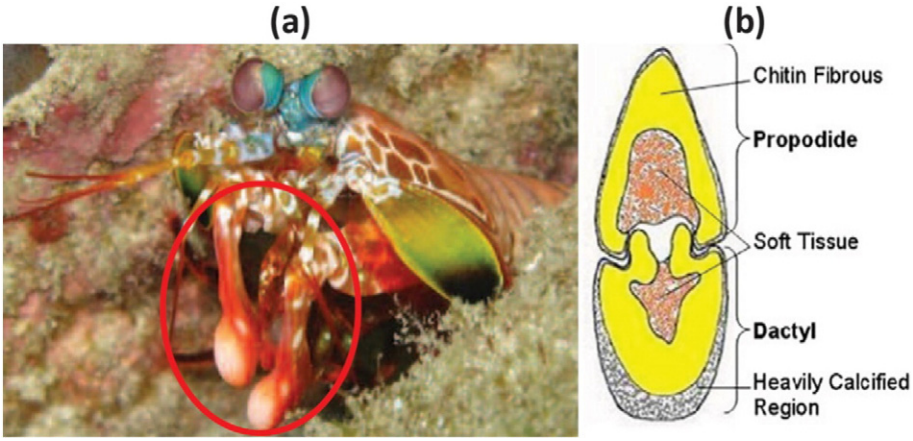

Fig. 29. Mantis shrimp (*Gonodactylus chiragra*) dactyl club. (a) A mantis shrimp with the dactyl clubs circled; (b) diagram of the cross-section of the dactyl club showing the heavily calcified surface, the fibrous chitin in the interior and soft tissue at the core.
Adapted from: (a) [205], (b) [4].

- Pierce resistant body armor based upon the overlapping protection of fish scales [56]: perhaps the most common marine organism bioinspiration source, these armors date back to the scaled armor of the Roman Empire, the "Lorica Squamata" (Fig. 30a) [48]. This armor consisted of individual, overlapping metal scales (called "squamae") set over a leather shirt, thus providing both a hard penetration resistant surface and a tough energy absorbent base. Modern examples of fish inspired armor include the recently developed "Dragon Skin" armor that consists of circular, ceramic, bulletproof plates oriented in overlapping arrays within a wearable vest (Fig. 30b) [13,48].
- Impact resistant fiber composites based upon the dactyl club of the mantis shrimp [208]: these carbon fiber-epoxy composites are fabricated to mimic the helical structural design of the dactyl club. Similar to the mantis shrimp itself, when impacted, these bioinspired composites can reduce the through-thickness damage propagation.

Given the specific environments that marine organisms have evolved in, there is still much room for bioinspiration in fields such as high pressure applications (deep sea organisms), filtration (gills) and high strength wet-adhesives (organisms in tidal zones that must adhere and resist the force of waves). Additionally, with 91% of marine organisms yet to be discovered and classified [8], the wealth of knowledge to provide bioinspiration will only continue to grow.

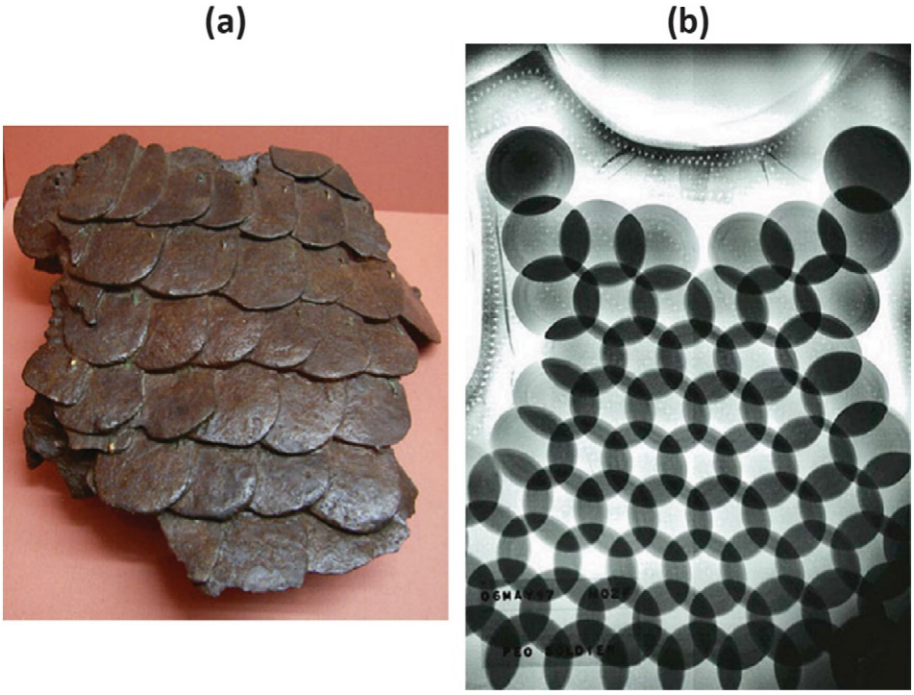

Fig. 30. Bioinspired armor designs based upon fish scales. (a) Ancient Roman "Lorica Squamata" armor designed with metal overlapping scales over a leather shirt; (b) modern "Dragon Skin" armor designed with ceramic, bulletproof and overlapping plates.
Adapted from [48].

8. Conclusions

From the wide range of marine organisms covered within this review, it is possible to make some conclusions on the qualities that contribute to specific forms of defense:

1. Crushing resistant structures: The majority of organisms that focus on crushing resistance opt for relatively high mineral content within their defenses in order to increase strength. Given this, ingenious methods are employed to increase ductility and/or toughness, including the brick-and-mortar structure of mollusk nacre, the helical fiber arrangement in crustacean exoskeletons, the geometric macrostructures of diatoms and the sliding plates of the seahorse.
2. Flexure resistant structures: Organisms that aim to provide flexure resistance tend to still require high strength and therefore often place a focus on strategic allocation of material, as is the case in the precisely aligned spicules of the sea sponge and the porous/dense layers in the spines of sea urchins.
3. Piercing resistant structures: Structures focused upon pierce resistance must provide both hardness to halt penetration and toughness to absorb the force of a bite. In most cases this is achieved through a layered structure, as is found in many fish scales, scutes and marine skeletal armors, with a rigid surface plate supported by a tough base.
4. Impact resistant structures: The impact resistant dactyl clubs of the mantis shrimp employ a rigid outer layer and a helical energy absorbent inner layer. The gradient in mechanical properties between these two layers is itself an effective mechanism to absorb energy and deflect cracks.

The oceans offer unique challenges to their inhabitants. From the inky darkness and extreme pressures of the ocean floor to the immense forces of crashing waves at the shorelines, organisms have evolved different strategies to survive and thrive under these extreme conditions. In contrast to terrestrial organisms, marine organisms have adapted different protective mechanisms, shaped by the specific effects of hydrostatic pressure, local temperature and salinity, motion from currents and swells and complete hydration. These defensive mechanisms take on many different forms with both passive (e.g. diatom exoskeletons and mollusk shells) and active (e.g. porcupine fish and sea urchin spines) mechanisms represented. As with all biological materials, the sheer complexity of structures that are formed from relatively simple constituents of biominerals (carbonated hydroxyapatite, calcium carbonate, amorphous silica, magnetite and iron sulfide) and biopolymers (collagen, keratin, chitin and cartilage) is astounding. Additionally, these complex structures provide for all manner of bioinspired designs, from fiber optics to body armor, which have real-world impact. While this review has served as an introduction to many marine biological materials that have been studied, there are still many material secrets of marine life yet to be cracked.

Acknowledgments

This work is supported by a Multi-University Research Initiative through the Air Force Office of Scientific Research (AFOSR-FA9550-15-1-0009) (S.E.N., M.A.M. and J.M.), Scripps Institution of Oceanography (J.R.A.T.) and the Department of Mechanical Engineering, College of Engineering and Science, Clemson University (M.M.P.). The authors wish to thank Prof. Lisa Levin and Kirk Sato of Scripps Institution of Oceanography as well as Michael Frank of the University of California, San Diego for their input on Echinodermata, Frances Su and Esther Cory of the University of California, San Diego for their input on Diodontidae, Haochan Quan of the University of California, San Diego for his input on the coelacanth, Dr. James Tyler of the Smithsonian Institute for his input on fish scutes and spines, Prof. Phil Hastings of the Scripps Institution of Oceanography for his input on marine biology and Prof. Cheryl Hayashi of the University of California, Riverside for her input on biological classifications.

References

[1] E. Arzt, Biological and artificial attachment devices: lessons for materials scientists from flies and geckos, Mater. Sci. Eng. C 26 (2006) 1245–1250.
[2] M.A. Meyers, J. McKittrick, P.-Y. Chen, Structural biological materials: critical mechanics-materials connections, Science 339 (2013) 773–779.
[3] M.A. Meyers, P.-Y. Chen, M.I. Lopez, Y. Seki, A.Y.M. Lin, Biological materials: a materials science approach, J. Mech. Behav. Biomed. Mater. 4 (2011) 626–657.
[4] M.A. Meyers, P.-Y. Chen, A.Y.M. Lin, Y. Seki, Biological materials: structure and mechanical properties, Prog. Mater. Sci. 53 (2008) 1–206.
[5] P.-Y. Chen, J. McKittrick, M.A. Meyers, Biological materials: functional adaptations and bioinspired designs, Prog. Mater. Sci. 57 (2012) 1492–1704.
[6] S.E. Naleway, M.M. Porter, J. McKittrick, M.A. Meyers, Structural design elements in biological materials: application to bioinspiration, Adv. Mater. 27 (2015) 5455–5476.
[7] U.G.K. Wegst, M.F. Ashby, The mechanical efficiency of natural materials, Philos. Mag. 84 (2004) 2167–2181.
[8] C. Mora, D.P. Tittensor, S. Adl, A.G.B. Simpson, B. Worm, How many species are there on earth and in the ocean? PLoS One 9 (2011), e1001127.
[9] E. Munch, M.E. Launey, D.H. Alsem, E. Saiz, A.P. Tomsia, R.O. Ritchie, Tough, bio-inspired hybrid materials, Science 322 (2008) 1516–1520.
[10] W.E.G. Müller, X.H. Wang, F.Z. Cui, K.P. Jochum, W. Tremel, J. Bill, H.C. Schroder, F. Natalio, U. Schlossmacher, M. Wiens, Sponge spicules as blueprints for the biofabrication of inorganic–organic composites and biomaterials, Appl. Microbiol. Biotechnol. 83 (2009) 397–413.
[11] J. Aizenberg, V.C. Sundar, A.D. Yablon, J.C. Weaver, G. Chen, Biological glass fibers: correlation between optical and structural properties, Proc. Natl. Acad. Sci. 101 (2004) 3358–3363.
[12] W. Yang, S.E. Naleway, M.M. Porter, M.A. Meyers, J. McKittrick, The armored carapace of the boxfish, Acta Biomater. 23 (2015) 1–10.
[13] W. Yang, I.H. Chen, B. Gludovatz, E.A. Zimmermann, R.O. Ritchie, M.A. Meyers, Natural flexible dermal armor, Adv. Mater. 25 (2013) 31–48.
[14] R.O. Ritchie, The conflicts between strength and toughness, Nat. Mater. 10 (2011) 817–822.
[15] J.D. Currey, K. Brear, Hardness, young's modulus and yield stress in mammalian mineralized tissues, J. Mater. Sci. Mater. Med. 1 (1990) 14–20.
[16] R. Parenteau-Bareil, R. Gauvin, F. Berthod, Collagen-based biomaterials for tissue engineering applications, Materials 3 (2010) 1863–1887.
[17] Y. Omura, N. Urano, S. Kimura, Occurrence of fibrillar collagen with structure of (alpha(1))(2) alpha(2) in the test of sea urchin *Asthenosoma ijimai*, Comp. Biochem. Physiol. B 115 (1996) 63–68.
[18] T. Nagai, N. Suzuki, Partial characterization of collagen from purple sea urchin (*Anthocidaris crassispina*) test, Int. J. Food Sci. Technol. 35 (2000) 497–501.
[19] S. Kimura, Y. Takema, M. Kubota, Octopus skin collagen — isolation and characterization of collagen comprising two distinct a chains, J. Biol. Chem. 256 (1981) 3230–3234.
[20] S. Kimura, Y. Omura, M. Ishida, H. Shirai, Molecular characterization of fibrillar collagen from the body wall of starfish *Asterias amurenis*, Comp. Biochem. Physiol. B 104 (1993) 663–668.
[21] S. Kimura, S. Miura, Y.H. Park, Collagen as the major edible component of jellyfish (*Stomolophus nomural*), J. Food Sci. 48 (1983) 1758–1760.
[22] S. Miura, S. Kimura, Jellyfish mesogloea collagen. Characterization of molecules as α1 α2 α3 heterotrimers, J. Biol. Chem. 260 (1985) 5352–5356.
[23] S. Kimura, X.P. Zhu, R. Matsui, M. Shijoh, S. Takamizawa, Characterization of fish muscle type-I collagen, J. Food Sci. 53 (1988) 1315–1318.
[24] T. Nagai, Y. Araki, N. Suzuki, Collagen of the skin of ocellate puffer fish (*Takifugu rubripes*), Food Chem. 78 (2002) 173–177.
[25] M.A. Meyers, Y.S. Lin, E.A. Olevsky, P.-Y. Chen, Battle in the Amazon: *Arapaima* versus piranha, Adv. Biomater. 14 (2012) B88–B279.
[26] M.P.E. Wenger, L. Bozec, M.A. Horton, P. Masquida, Mechanical properties of collagen fibrils, Biophys. J. 93 (2007) 1255–1263.
[27] J.S. Graham, A.N. Vomund, C.L. Phillips, M. Grandbois, Structural changes in human type I collagen fibrils investigated by force spectroscopy, Exp. Cell Res. 299 (2004) 335–342.
[28] H. Ehrlich, Chitin and collagen as universal and alternative templates in biomineralization, Int. Geol. Rev. 52 (2010) 661–699.
[29] W. Yang, V.R. Sherman, B. Gludovatz, M. Mackey, E.A. Zimmermann, E.H. Chang, E. Schaible, Z. Qin, M.J. Buehler, R.O. Ritchie, M.A. Meyers, Protective role of *Arapaima* gigas fish scales: structure and mechanical behavior, Acta Biomater. 10 (2014) 3599–3614.
[30] J. McKittrick, P.-Y. Chen, S.G. Bodde, W. Yang, E.E. Novitskaya, M.A. Meyers, The structure, functions, and mechanical properties of keratin, JOM 64 (2012) 449–468.
[31] J.G. Rouse, M.E. Van Dyke, A review of keratin-based biomaterials for biomedical applications, Materials 3 (2010) 999–1014.
[32] E.A. Koch, R.H. Spitzer, R.B. Pithawalla, F.A. Castillos, Hagfish biopolymer: a type I/type II homologue of epidermal keratin intermediate filaments, Int. J. Biol. Macromol. 17 (1995) 283–292.
[33] M. Feughelman, Structural features of keratin suggested by its mechanical properties, Biochim. Biophys. Acta 32 (1959) 596–597.
[34] R.D.B. Fraser, T.P. MacRae, D.A.D. Parry, E. Suzuki, Structure of beta-keratin, Polymer 10 (1969) 810.
[35] M.W. Trim, M.F. Horstemeyer, H. Rhee, H. Le Kadiri, L.N. Williams, J. Liao, K.B. Walters, J. McKittrick, S.J. Park, The effects of water and microstructure on the mechanical properties of bighorn sheep (*Ovis canadensis*) horn keratin, Acta Biomater. 7 (2011) 1228–1240.

[36] L. Tombolato, E.E. Novitskaya, P.-Y. Chen, F.A. Sheppard, J. McKittrick, Microstructure, elastic properties and deformation mechanisms of horn keratin, Acta Biomater. 6 (2010) 319–330.
[37] H. Zahn, J. Fohles, M. Nienhaus, A. Schwan, M. Spel, Wool as a biological composite structure, Ind. Eng. Chem. Prod. Res. Dev. 19 (1980) 496–501.
[38] S.L. Rosen, Fundamental Principles of Polymeric Materials, 2nd ed. John Wiley & Sons Inc., New York, 1993.
[39] M.A. Kennedy, A.J. Peacock, L. Mandelkern, Tensile properties of crystalline polymers — linear polyethylene, Macromolecules 27 (1994) 5297–5310.
[40] M.N.V.R. Kumar, A review of chitin and chitosan applications, React. Funct. Polym. 46 (2000) 1–27.
[41] M. Rinaudo, Chitin and chitosan: properties and applications, Prog. Polym. Sci. 31 (2006) 603–632.
[42] A. Miserez, D. Rubin, J.H. Waite, Cross-linking chemistry of squid beak, J. Biol. Chem. 285 (2010) 38115–38124.
[43] K.M. Rudall, W. Kenchington, The chitin system, Biol. Rev. 48 (1973) 597–633.
[44] Y. Bouligand, Twisted fiberous arrangements in biological materials and cholesteric mesophases, Tissue Cell 4 (1972) 189–217.
[45] M.M. Giraud-Guille, Fine structure of the chitin protein system in the crab cuticle, Tissue Cell 16 (1984) 75–92.
[46] M.M. Giraud-Guille, H. Chanzy, R. Vuong, Chitin crystals in arthropod cuticles revealed by diffraction contrast transmission electron-microscopy, J. Struct. Biol. 103 (1990) 232–240.
[47] M.M. Giraud-Guille, Plywood structures in nature, Curr. Opin. Solid State Mater. Sci. 3 (1998) 221–227.
[48] H. Ehrlich, Biological Materials of Marine Origin: Springer, 2015.
[49] M.N. Dean, A.P. Summers, Mineralized cartilage in the skeleton of chondrichthyan fishes, Zoology 109 (2006) 164–168.
[50] A.G. Cole, B.K. Hall, Cartilage differentiation in cephalopod molluscs, Zoology 112 (2009) 2–15.
[51] A.G. Cole, B.K. Hall, The nature and significance of invertebrate cartilages revisited: distribution and histology of cartilage and cartilage-like tissues within the Metazoa, Zoology 107 (2004) 261–273.
[52] P.-Y. Chen, D. Toroian, P.A. Price, J. McKittrick, Minerals form a continuum phase in mature cancellous bone, Calcif. Tissue Int. 88 (2011) 351–361.
[53] S.V. Dorozhkin, Calcium orthophosphates in nature, biology and medicine, Materials 2 (2009) 399–498.
[54] S. Weiner, H.D. Wagner, The material bone: structure mechanical function relations, Annu. Rev. Mater. Sci. 28 (1998) 271–298.
[55] E.E. Novitskaya, P.-Y. Chen, S. Lee, A.B. Castro-Cesena, G.A. Hirata, V.A. Lubarda, J. McKittrick, Anisotropy in the compressive mechanical properties of bovine cortical bone and the mineral and protein constituents, Acta Biomater. 7 (2011) 3170–3177.
[56] W. Yang, I.H. Chen, J. McKittrick, M.A. Meyers, Flexible dermal armor in nature, JOM 64 (2012) 475–485.
[57] M.M. Porter, J. McKittrick, M.A. Meyers, Biomimetic materials by freeze casting, JOM 65 (2013) 720–727.
[58] M. Vallet-Regi, J.M. Gonzalez-Calbet, Calcium phosphates as substitution of bone tissues, Prog. Solid State Chem. 32 (2004) 1–31.
[59] L.L. Hench, Bioceramics — from concept to clinic, J. Am. Ceram. Soc. 74 (1991) 1487–1510.
[60] L.L. Hench, Bioceramics, J. Am. Ceram. Soc. 81 (1998) 1705–1728.
[61] S. Deville, E. Saiz, R.K. Nalla, A.P. Tomsia, Freezing as a path to build complex composites, Science 311 (2006) 515–518.
[62] M.J. Olszta, X.G. Cheng, S.S. Jee, R. Kumar, Y.Y. Kim, M.J. Kaufman, E.P. Douglas, L.B. Gower, Bone structure and formation: a new perspective, Mater. Sci. Eng. R 58 (2007) 77–116.
[63] F. Nudelman, K. Pieterse, A. George, P.H.H. Bomans, H. Friedrich, L.J. Brylka, P.A.J. Hilbers, G. de With, N.A.J.M. Sommerdijk, The role of collagen in bone apatite formation in the presence of hydroxyapatite nucleation inhibitors, Nat. Mater. 9 (2010) 1004–1009.
[64] T. Ikoma, H. Kobayashi, J. Tanaka, D. Walsh, S. Mann, Microstructure, mechanical, and biomimetic properties of fish scales from *Pagrus major*, J. Struct. Biol. 142 (2003) 327–333.
[65] P. Ducheyne, Q. Qiu, Bioactive ceramics: the effect of surface reactivity on bone formation and bone cell function, Biomaterials 20 (1999) 2287–2303.
[66] G. Mayer, Rigid biological systems as models for synthetic composites, Science 310 (2005) 1144–1147.
[67] S. Blank, M. Arnoldi, S. Khoshnavaz, L. Treccani, M. Kuntz, K. Mann, G. Grathwohl, M. Fritz, The nacre protein perlucin nucleates growth of calcium carbonate crystals, J. Microsc. (Oxford) 212 (2003) 280–291.
[68] F.C. Meldrum, H. Colfen, Controlling mineral morphologies and structures in biological and synthetic systems, Chem. Rev. 108 (2008) 4332–4432.
[69] G. Wolf, E. Konigsberger, H.G. Schmidt, L.C. Konigsberger, H. Gamsjager, Thermodynamic aspects of the vaterite-calcite phase transition, J. Therm. Anal. Calorim. 60 (2000) 463–472.
[70] G. Falini, S. Albeck, S. Weiner, L. Addadi, Control of aragonite or calcite polymorphism by mollusk shell macromolecules, Science 271 (1996) 67–69.
[71] A.M. Belcher, X.H. Wu, R.J. Christensen, P.K. Hansma, G.D. Stucky, D.E. Morse, Control of crystal phase switching and orientation by soluble mollusc-shell proteins, Nature 381 (1996) 56–58.
[72] X. Long, Y.R. Ma, L.M. Qi, Biogenic and synthetic high magnesium calcite — a review, J. Struct. Biol. 185 (2014) 1–14.
[73] G. Falini, S. Fermani, M. Gazzano, A. Ripamonti, Biomimetic crystallization of calcium carbonate polymorphs by means of collagenous matrices, Chem. Eur. J. 3 (1997) 1807–1814.
[74] R.M.S. Schofield, J.C. Niedbala, M.H. Nesson, Y. Tao, J.E. Shokes, R.A. Scott, M.J. Latimer, Br-rich tips of calcified crab claws are less hard but more fracture resistant: a comparison of mineralized and heavy-element biological materials, J. Struct. Biol. 166 (2009) 272–287.
[75] B.W. Cribb, A. Rathmell, R. Charters, R. Rasch, H. Huang, I.R. Tibbetts, Structure, composition and properties of naturally occurring non-calcified crustacean cuticle, Arthropod Struct. Dev. 38 (2009) 173–178.
[76] C.C. Perry, T. Keeling-Tucker, Biosilicification: the role of the organic matrix in structure control, J. Biol. Inorg. Chem. 5 (2000) 537–550.
[77] E. Epstein, Silicon: its manifold roles in plants, Ann. Appl. Biol. 155 (2009) 155–160.
[78] P.W. Lucas, I.M. Turner, N.J. Dominy, N. Yamashita, Mechanical defences to herbivory, Ann. Bot. 86 (2000) 913–920.
[79] I.C. Gebeshuber, J.H. Kindt, J.B. Thompson, Y. Del Amo, H. Stachelberger, M.A. Brzezinski, G.D. Stucky, D.E. Morse, P.K. Hansma, Atomic force microscopy study of living diatoms in ambient conditions, J. Microsc. (Oxford) 212 (2003) 292–299.
[80] A.P. Garcia, N. Pugno, M.J. Buehler, Superductile, wavy silica nanostructures inspired by diatom algae, Adv. Eng. Mater. 13 (2011) B14–B405.
[81] E. Epstein, Silicon, Annu. Rev. Plant Physiol. Plant Mol. Biol. 50 (1999) 641–664.
[82] K. Shimizu, J. Cha, G.D. Stucky, D.E. Morse, Silicatein alpha: cathepsin L-like protein in sponge biosilica, Proc. Natl. Acad. Sci. U. S. A. 95 (1998) 6234–6238.
[83] L. Xia, Y. Liu, Z.B. Li, Biosilicification templated by amphiphilic block copolypeptide assemblies, Macromol. Biosci. 10 (2010) 1566–1575.
[84] D. Schuler, R.B. Frankel, Bacterial magnetosomes: microbiology, biomineralization and biotechnological applications, Appl. Microbiol. Biotechnol. 52 (1999) 464–473.
[85] C.T. Lefevre, N. Viloria, M.L. Schmidt, M. Posfai, R.B. Frankel, D.A. Bazylinski, Novel magnetite-producing magnetotactic bacteria belonging to the Gammaproteobacteria, ISME J. 6 (2012) 440–450.
[86] K.J. Lohmann, Magnetic orientation by hatchling loggerheasd sea-turtles (*Caretta caretta*), J. Exp. Biol. 155 (1991) 37–49.
[87] K.J. Lohmann, C.M.F. Lohmann, Detection of magnetic field intensity by sea turtles, Nature 380 (1996) 59–61.
[88] L.C. Boles, K.J. Lohmann, True navigation and magnetic maps in spiny lobsters, Nature 421 (2003) 60–63.
[89] Q.Q. Wang, M. Nemoto, D.S. Li, J.C. Weaver, B. Weden, J. Stegemeier, K.N. Bozhilov, L.R. Wood, G.W. Milliron, C.S. Kim, E. DiMasi, D. Kisailus, Phase transformations and structural developments in the radular teeth of *Cryptochiton stelleri*, Adv. Funct. Mater. 23 (2013) 2908–2917.
[90] S.E. Greene, A. Komeili, Biogenesis and subcellular organization of the magnetosome organelles of magnetotactic bacteria, Curr. Opin. Cell Biol. 24 (2012) 490–495.
[91] G.W. Luther, T.F. Rozan, M. Taillefert, D.B. Nuzzio, C. Di Meo, T.M. Shank, R.A. Lutz, S.C. Cary, Chemical speciation drives hydrothermal vent ecology, Nature 410 (2001) 813–816.
[92] Y. Suzuki, R.E. Kopp, T. Kogure, A. Suga, K. Takai, S. Tsuchida, N. Ozaki, K. Endo, J. Hashimoto, Y. Kato, C. Mizota, T. Hirata, H. Chiba, K.H. Nealson, K. Horikoshi, J.L. Kirschvink, Sclerite formation in the hydrothermal-vent "scaly-foot" gastropod — possible control of iron sulfide biomineralization by the animal, Earth Planet. Sci. Lett. 242 (2006) 39–50.
[93] F. Barthelat, H. Tang, P.D. Zavattieri, C.M. Li, H.D. Espinosa, On the mechanics of mother-of-pearl: a key feature in the material hierarchical structure, J. Mech. Phys. Solids 55 (2007) 306–337.
[94] H.D. Espinosa, A.L. Juster, F.J. Latourte, O.Y. Loh, D. Gregoire, P.D. Zavattieri, Tablet-level origin of toughening in abalone shells and translation to synthetic composite materials, Nat. Commun. 2 (2011).
[95] L. Addadi, D. Joester, F. Nudelman, S. Weiner, Mollusk shell formation: a source of new concepts for understanding biomineralization processes, Chemistry 12 (2006) 980–987.
[96] A.Y.M. Lin, M.A. Meyers, K.S. Vecchio, Mechanical properties and structure of *Strombus gigas*, *Tridacna gigas*, and *Haliotis rufescens* sea shells: a comparative study, Mater. Sci. Eng. C 26 (2006) 1380–1389.
[97] A.Y.M. Lin, P.-Y. Chen, M.A. Meyers, The growth of nacre in the abalone shell, Acta Biomater. 4 (2008) 131–138.
[98] A. Lin, M.A. Meyers, Growth and structure in abalone shell, Mater. Sci. Eng. A 390 (2005) 27–41.
[99] M.A. Meyers, C.T. Lim, A. Li, B.R.H. Nizam, E.P.S. Tan, Y. Seki, J. McKittrick, The role of organic intertile layer in abalone nacre, Mater. Sci. Eng. C 29 (2009) 2398–2410.
[100] M.I. Lopez, P.E.M. Martinez, M.A. Meyers, Organic interlamellar layers, mesolayers and mineral nanobridges: contribution to strength in abalone (*Haliotis rufescence*) nacre, Acta Biomater. 10 (2014) 2056–2064.
[101] M.I. Lopez, P.-Y. Chen, J. McKittrick, M.A. Meyers, Growth of nacre in abalone: seasonal and feeding effects, Mater. Sci. Eng. C 31 (2011) 238–245.
[102] R. Menig, M.H. Meyers, M.A. Meyers, K.S. Vecchio, Quasi-static and dynamic mechanical response of *Haliotis rufescens* (abalone) shells, Acta Mater. 48 (2000) 2383–2393.
[103] C. Salinas, D. Kisailus, Fracture mitigation strategies in gastropod shells, JOM 65 (2013) 473–480.
[104] R. Menig, M.H. Meyers, M.A. Meyers, K.S. Vecchio, Quasi-static and dynamic mechanical response of *Strombus gigas* (conch) shells, Mater. Sci. Eng. A 297 (2001) 203–211.
[105] S. Kamat, X. Su, R. Ballarini, A.H. Heuer, Structural basis for the fracture toughness of the shell of the conch *Strombus gigas*, Nature 405 (2000) 1036–1040.
[106] R.O. Ritchie, Mechanisms of fatigue crack-propagation in metals, ceramics and composites — role of crack tip sheilding, Mater. Sci. Eng. A 103 (1988) 15–28.
[107] R.O. Ritchie, Mechanisms of fatigue-crack propagation in ductile and brittle solids, Int. J. Fract. 100 (1999) 55–83.

[108] F. Bouville, E. Maire, S. Meille, B. Van de Moortele, A.J. Stevenson, S. Deville, Strong, tough and stiff bioinspired ceramics from brittle constituents, Nat. Mater. 13 (2014) 508–514.
[109] H.M. Yao, M. Dao, T. Imholt, J.M. Huang, K. Wheeler, A. Bonilla, S. Suresh, C. Ortiz, Protection mechanisms of the iron-plated armor of a deep-sea hydrothermal vent gastropod, PNAS 107 (2010) 987–992.
[110] A. Waren, S. Bengtson, S.K. Goffredi, C.L. Van Dover, A hot-vent gastropod with iron sulfide dermal sclerites, Science 302 (2003) 1007.
[111] M.J. Vendrasco, T.E. Wood, B.N. Runnegar, Articulated Palaeozoic fossil with 17 plates greatly expands disparity of early chitons, Nature 429 (2004) 288–291.
[112] K. Treves, W. Traub, S. Weiner, L. Addadi, Aragonite formation in the chiton (*Mollusca*) girdle, Helv. Chim. Acta 86 (2003) 1101–1112.
[113] M.J. Connors, H. Ehrlich, M. Hog, C. Godeffroy, S. Araya, I. Kallai, D. Gazit, M. Boyce, C. Ortiz, Three-dimensional structure of the shell plate assembly of the chiton *Tonicella marmorea* and its biomechanical consequences, J. Struct. Biol. 177 (2012) 314.
[114] M. Nemoto, Q.Q. Wang, D.S. Li, S.Q. Pan, T. Matsunaga, D. Kisailus, Proteomic analysis from the mineralized radular teeth of the giant Pacific chiton, *Cryptochiton stelleri* (Mollusca), Proteomics 12 (2012) 2890–2894.
[115] K.M. Towe, H.A. Lowensta, Ultrastructure and development of iron mineralization in radular teeth of *Cryptochiton stelleri* (Mollusca), J. Ultrastruct. Res. 17 (1967) 1–13.
[116] L.M. Gordon, J.K. Roman, R.M. Everly, M.J. Cohen, J.J. Wilker, D. Joester, Selective formation of metastable ferrihydrite in the chiton tooth, Angew. Chem. 53 (2014) 11506–11509.
[117] V. Martin-Jezequel, M. Hildebrand, M.A. Brzezinski, Silicon metabolism in diatoms: implications for growth, J. Phycol. 36 (2000) 821–840.
[118] M. Hildebrand, Diatoms, biomineralization processes, and genomics, Chem. Rev. 108 (2008) 4855–4874.
[119] G. Sarthou, K.R. Timmermans, S. Blain, P. Treguer, Growth physiology and fate of diatoms in the ocean: a review, J. Sea Res. 53 (2005) 25–42.
[120] P. Treguer, D.M. Nelson, A.J. Van Beenekom, D.J. DeMaster, A. Leynaert, B. Queguiner, The silica balance in the world ocean: a reestimate, Science 268 (1995) 375–379.
[121] C.E. Hamm, R. Merkel, O. Springer, P. Jurkojc, C. Maier, K. Prechtel, V. Smetacek, Architecture and material properties of diatom shells provide effective mechanical protection, Nature 421 (2003) 841–843.
[122] H. Hildebrand, C.D. Durselen, D. Kirschtel, U. Pollingher, T. Zohary, Biovolume calculation for pelagic and benthic microalgae, J. Phycol. 35 (1999) 403–424.
[123] D. Losic, K. Short, J.G. Mitchell, R. Lal, N.H. Voelcker, AFM nanoindentations of diatom biosilica surfaces, Langmuir 23 (2007) 5014–5021.
[124] N. Almqvist, Y. Delamo, B.L. Smith, N.H. Thomson, A. Bartholdson, R. Lal, M. Brzezinski, P.K. Hansma, Micromechanical and structural properties of a pennate diatom investigated by atomic force microscopy, J. Microsc. 202 (2001) 518–532.
[125] G. Francius, B. Tesson, E. Dague, V. Martin-Jezequel, Y.F. Dufrene, Nanostructure and nanomechanics of live *Phaeodactylum tricornutum* morphotypes, Environ. Microbiol. 10 (2008) 1344–1356.
[126] N. Kroger, R. Deutzmann, C. Bergsdorf, M. Sumper, Species-specific polyamines from diatoms control silica morphology, PNAS 97 (2000) 14133–14138.
[127] N. Kroger, R. Deutzmann, M. Sumper, Polycationic peptides from diatom biosilica that direct silica nanosphere formation, Science 286 (1999) 1129–1132.
[128] M. Sumper, A phase separation model for the nanopatterning of diatom biosilica, Science 295 (2002) 2430–2433.
[129] J.R. Young, Functions of coccoliths, in: W.G. Siesser, A. Winter (Eds.), Coccolithophores, Cambridge University Press, Cambridge, UK 1994, pp. 63–82.
[130] B.L. Smith, G.T. Paloczi, P.K. Hansma, R.P. Levine, Discerning nature's mechanism for making complex biocomposite crystals, J. Cryst. Growth 211 (2000) 116–121.
[131] S. Mann, N.H.C. Sparks, Single crystal nature of coccolith elements of the marine alga *Emiliania huxleyi* as determined by electron diffraction and high resolution electron microscopy, Proc. R. Soc. B 234 (1988) 441–453.
[132] M.E. Marsh, Regulation of $CaCO_3$ formation in coccolithophores, Comp. Biochem. Physiol. B 136 (2003) 743–754.
[133] P.-Y. Chen, A.Y.M. Lin, J. McKittrick, M.A. Meyers, Structure and mechanical properties of crab exoskeletons, Acta Biomater. 4 (2008) 587–596.
[134] D.F. Travis, The molting cycle of the spiny lobster, *Panulirus argus*-Latreille. II. Pre-ecdysial histological and histochemical changes in the hepatopancreas and integumental tissues, Biol. Bull. 108 (1955) 88–112.
[135] Y. Bouligand, Aspects ultrastructuraux de la calcification chez les Crabes, Septieme Congres Internationale de Microscopie Electronique, Gernoble, France, 1970 105–106.
[136] H.O. Fabritius, C. Sachs, P.R. Triguero, D. Raabe, Influence of structural principles on the mechanics of a biological fiber-based composite material with hierarchical organization: the exoskeleton of the lobster *Homarus americanus*, Adv. Mater. 21 (2009) 391–400.
[137] D. Raabe, C. Sachs, P. Romano, The crustacean exoskeleton as an example of a structurally and mechanically graded biological nanocomposite material, Acta Mater. 53 (2005) 4281–4292.
[138] R. Dillaman, S. Hequembourg, M. Gay, Early pattern of calcification in the dorsal carapace of the blue crab, *Callinectes sapidus*, J. Microsc. 263 (2005) 356–374.
[139] H.O. Fabritius, E.S. Karsten, K. Balasundaram, S. Hild, K. Huemer, D. Raabe, Correlation of structure, composition and local mechanical properties in the dorsal carapace of the edible crab *Cancer pagurus*, Z. Krist. Cryst. Mater. 227 (2012) 766–776.
[140] D. Raabe, P. Romano, C. Sachs, H. Fabritius, A. Al-Sawalmih, S. Yi, G. Servos, H.G. Hartwig, Microstructure and crystallographic texture of the chitin-protein network in the biological composite material of the exoskeleton of the lobster *Homarus americanus*, Mater. Sci. Eng. A 421 (2006) 143–153.
[141] L. Cheng, L.Y. Wang, A.M. Karlsson, Image analyses of two crustacean exoskeletons and implications of the exoskeletal microstructure on the mechanical behavior, J. Mater. Res. 23 (2008) 2854–2872.
[142] C. Sachs, H. Fabritius, D. Raabe, Experimental investigation of the elastic–plastic deformation of mineralized lobster cuticle by digital image correlation, J. Struct. Biol. 155 (2006) 409–425.
[143] H.R. Hepburn, I. Joffe, N. Green, K.J. Nelson, Mechanical-properties of a crab shell, Comp. Biochem. Physiol. 50 (1975) 551–554.
[144] I. Joffe, H.R. Hepburn, K.J. Nelson, N. Green, Mechanical-properties of a crustacean exoskelton, Comp. Biochem. Physiol. 50 (1975) 545–549.
[145] C.L. Williams, R.M. Dillaman, E.A. Elliott, D.M. Gay, Formation of the arthrodial membrane in the blue crab, *Callinectes sapidus*, J. Morphol. 256 (2003) 260–269.
[146] C.A. Melnick, Z. Chen, J.J. Mecholsky, Hardness and toughness of exoskeleton material in the stone crab, *Menippe mercenaria*, J. Mater. Res. 11 (1996) 2903–2907.
[147] S.J. Foster, A.C.J. Vincent, Life history and ecology of seahorses: implications for conservation and management, J. Fish Biol. 65 (2004) 1–61.
[148] T.R. Consi, P.A. Seifert, M.S. Triantafyllou, E.R. Edelman, The dorsal fin engine of the seahorse, Hippocampus 248 (2001) 1.
[149] M.A. Ashley-Ross, Mechanical properties of the dorsal fin muscle of seahorse (*Hippocampus*) and pipefish (*Syngnathus*), J. Exp. Zool. 293 (2002) 561–577.
[150] M.M. Porter, E.E. Novitskaya, A.B. Castro-Cesena, M.A. Meyers, J. McKittrick, Highly deformable bones: unusual deformation mechanisms of seahorse armor, Acta Biomater. 9 (2013) 6763–6770.
[151] M.E. Hale, Functional morphology of ventral tail bending and prehensile abilities of the seahorse, *Hippocampus kuda*, J. Morphol. 227 (1996) 51–65.
[152] T. Praet, D. Adriaens, S. Van Cauter, B. Masschaele, M. De Beule, B. Verhegghe, Inspiration from nature: dynamic modelling of the musculoskeletal structure of the seahorse tail, Int. J. Numer. Methods Biomed. Eng. 28 (2012) 1028–1042.
[153] C. Neutens, D. Adriaens, J. Christiaens, B. De Kegel, M. Dierick, R. Boistel, L. Van Hoorebeke, Grasping convergent evolution in syngnathids: a unique tale of tails, J. Anat. 224 (2014) 710–723.
[154] M.M. Porter, D. Adriaens, R.L. Hatton, M.A. Meyers, J. McKittrick, Why the seahorse tail is square, Science 349 (2015) 6683 (aaa).
[155] D. Kleiber, L.K. Blight, I.R. Caldwell, A.C.J. Vincent, The importance of seahorses and pipefishes in the diet of marine animals, Rev. Fish Biol. Fish. 21 (2011) 205–223.
[156] W.E.G. Müller, X.H. Wang, K. Kropf, H. Ushijima, W. Geurtsen, C. Eckert, M.N. Tahir, W. Tremel, A. Boreiko, U. Schloßmacher, J.H. Li, H.C. Schröder, Bioorganic/inorganic hybrid composition of sponge spicules: matrix of the giant spicules and of the comitalia of the deep sea hexactinellid Monorhaphis, J. Struct. Biol. 161 (2008) 188–203.
[157] J.C. Weaver, J. Aizenberg, G.E. Fantner, D. Kisailus, A. Woesz, P. Allen, K. Fields, M.J. Porter, F.W. Zok, P.K. Hansma, P. Fratzl, D.E. Morse, Hierarchical assembly of the siliceous skeletal lattice of the hexactinellid sponge *Euplectella aspergillum*, J. Struct. Biol. 158 (2007) 93–106.
[158] J. Aizenberg, J.C. Weaver, M.S. Thanawala, V.C. Sundar, D.E. Morse, P. Fratzl, Skeleton of *Euplectella* sp.: structural hierarchy from the nanoscale to the macroscale, Science 309 (2005) 275–278.
[159] G. Imsiecke, R.T. Steffen, M. Custodio, R. Borojevic, W. Muller, Formation of spicules by sclerocytes from the freshwater sponge *Ephydatia muelleri* in short-term cultures in vitro, In Vitro Cell. Dev. Biol. Anim. 31 (1995) 528–535.
[160] J.N. Cha, K. Shimizu, Y. Zhou, S.C. Christiansen, B.F. Chmelka, G.D. Stucky, D.E. Morse, Silicatein filaments and subunits from a marine sponge direct the polymerization of silica and silicones in vitro, Proc. Natl. Acad. Sci. U. S. A. 96 (1999) 361–365.
[161] A. Woesz, J.C. Weaver, M. Kazanci, Y. Dauphin, J. Aizenberg, D.E. Morse, P. Fratzl, Micromechanical properties of biological silica in skeletons of deep-sea sponges, J. Mater. Res. 21 (2006) 2068–2078.
[162] M.M. Porter, L. Meraz, A. Calderon, H. Choi, A. Chouhan, L. Wang, M.A. Meyers, J. McKittrick, Torsional properties of helix-reinforced composites fabricated by magnetic freeze casting, Compos. Struct. 119 (2015) 174–184.
[163] V. Presser, S. Schultheiss, C. Berthold, K.G. Nickel, Sea urchin spines as a model-system for permeable, light-weight ceramics with graceful failure behavior. Part I. Mechanical behavior of sea urchin spines under compression, J. Bionic Eng. 6 (2009) 203–213.
[164] J. Seto, Y.R. Ma, S.A. Davis, F. Meldrum, A. Gourrier, Y.Y. Kim, U. Schilde, M. Sztucki, M. Burghammer, S. Maltsev, C. Jager, H. Colfen, Structure–property relationships of a biological mesocrystal in the adult sea urchin spine, PNAS 109 (2012) 3699–3704.
[165] Y. Oaki, H. Imai, Nanoengineering in echinoderms: the emergence of morphology from nanobricks, Small 2 (2006) 66–70.
[166] J. Aizenberg, J. Hanson, T.F. Koetzle, S. Weiner, L. Addadi, Control of macromolecule distribution within synthetic and biogenic single calcite crystals, J. Am. Chem. Soc. 119 (1997) 881–886.
[167] Y. Politi, T. Arad, E. Klein, S. Weiner, L. Addadi, Sea urchin spine calcite forms via a transient amorphous calcium carbonate phase, Science 306 (2004) 1161–1164.
[168] C. Moureaux, A. Perez-Huerta, P. Compere, W. Zhu, T. Leloup, M. Cusack, P. Dubois, Structure, composition and mechanical relations to function in sea urchin spine, J. Struct. Biol. 170 (2010) 41–49.
[169] P.B. Edwards, T.A. Ebert, Plastic responses to limited food availability and spine damage in the sea urchin *Strongylocentrotus purpuratus* (Stimpson), J. Exp. Mar. Biol. Ecol. 145 (1991) 205–220.
[170] P. Dubois, L. Ameye, Regeneration of spines and pedicellariae in echinoderms: a review, Microsc. Res. Tech. 55 (2001) 427–437.
[171] L.J. Gibson, M.F. Ashby, Cellular Solids: Structure and Properties, Cambridge University Press, 1999.

[172] X. Su, S. Kamat, A.H. Heuer, The structure of sea urchin spines, large biogenic single crystals of calcite, J. Mater. Sci. 35 (2000) 5545–5551.
[173] J. Weber, R. Greer, B. Voight, E. White, R. Roy, Unusual strength properties of echinoderm calcite, J. Ultrastruct. Res. 26 (1969) 355–366.
[174] Y. Ma, B. Aichmayer, O. Paris, P. Fratzl, A. Meibom, R.A. Metzler, Y. Politi, L. Addadi, P.U.P.A. Gilbert, S. Weiner, The grinding tip of the sea urchin tooth exhibits exquisite control over calcite crystal orientation and Mg distribution, PNAS 106 (2009) 6048–6053.
[175] Y. Ma, S.R. Cohen, L. Addadi, S. Weiner, Sea urchin tooth design: an "all-calcite" polycrystalline reinforced fiber composite for grinding rocks, Adv. Mater. 20 (2008) 1555–1559.
[176] C.E. Killian, R.A. Metzler, Y. Gong, T.H. Churchill, I.C. Olson, V. Trubetskoy, M.B. Christensen, J.H. Fournelle, F. De Carlo, S. Cohen, J. Mahamid, A. Scholl, A. Young, A. Doran, F.H. Wilt, S.N. Coppersmith, P.U.P.A. Gilbert, Self-sharpening mechanism of the sea urchin tooth, Adv. Funct. Mater. 21 (2011) 682–690.
[177] J.C. Tyler, F. Santini, Review and reconstructions of the tetraodonitform fishes from the Eocene of Monte Bolca, Italy, with comments on related tertiary taxa, Studi e Ricerche sui Giacimenti Terziari di Bolca, Museo Civico di Storia Naturale di Verona, 9 2002, pp. 47–119.
[178] E.L. Brainerd, Puffer inflation: functional morphology of postcranial structures in *Diodon holocanthus* (Tetraodontiformes), J. Morphol. 220 (1994) 243–261.
[179] T. Ikoma, H. Kobayashi, J. Tanaka, D. Walsh, S. Mann, Physical properties of type I collagen extracted from fish scales of *Pagrus major* and *Oreochromis niloticas*, Int. J. Biol. Macromol. 32 (2003) 199–204.
[180] D. Zhu, C.F. Ortega, R. Motamedi, L. Szewciw, F. Vernerey, F. Barthelat, Structure and mechanical performance of a "modern" fish scale, Adv. Eng. Mater. 14 (2012) B94–B185.
[181] B.J.F. Bruet, J.H. Song, M.C. Boyce, C. Ortiz, Materials design principles of ancient fish armour, Nat. Mater. 7 (2008) 748–756.
[182] J.H. Song, C. Ortiz, M.C. Boyce, Threat-protection mechanics of an armored fish, J. Mech. Behav. Biomed. Mater. 4 (2011) 699–712.
[183] E.A. Zimmermann, B. Gludovatz, E. Schaible, N.K.N. Dave, W. Yang, M.A. Meyers, R.O. Ritchie, Mechanical adaptability of the Bouligand-type structure in natural dermal armour, Nat. Commun. 4 (2013) 2634.
[184] J.H. Long, M.E. Hale, M.J. McHenry, M.W. Westneat, Functions of fish skin: flexural stiffness and steady swimming of longnose gar *Lepisosteus osseus*, J. Exp. Biol. 199 (1996) 2139–2151.
[185] J.H. Long, B. Adcock, R.G. Root, Force transmission via axial tendons in undulating fish: a dynamic analysis, Comp. Biochem. Physiol. A Physiol. 133 (2002) 911–929.
[186] J.H. Long, T.J. Koob, K. Irving, K. Combie, V. Engel, N. Livingston, A. Lammert, J. Schumacher, Biomimetic evolutionary analysis: testing the adaptive value of vertebrate tail stiffness in autonomous swimming robots, J. Exp. Biol. 209 (2006) 4732–4746.
[187] W. Yang, B. Gludovatz, E.A. Zimmermann, H.A. Bale, R.O. Ritchie, M.A. Meyers, Structure and fracture resistance of alligator gar (*Atractosteus spatula*) armored fish scales, Acta Biomater. 9 (2013) 5876–5889.
[188] J.Y. Sire, A. Huysseune, Formation of dermal skeletal and dental tissues in fish: a comparative and evolutionary approach, Biol. Rev. 78 (2003) 219–249.
[189] E.S. Goodrich, On the scales of fish living and extinct, and then importance in classification, Proc. Zool. Soc. London 77 (1907) 751–774.
[190] F.J. Vernerey, F. Barthelat, Skin and scales of teleost fish: simple structure but high performance and multiple functions, J. Mech. Phys. Solids 68 (2014) 66–76.
[191] D.J. Zhu, L. Szewciw, F. Vernerey, F. Barthelat, Puncture resistance of the scaled skin from striped bass: collective mechanisms and inspiration for new flexible armor designs, J. Mech. Behav. Biomed. Mater. 24 (2013) 30–40.
[192] M.M. Smith, M.H. Hobdell, W.A. Miller, Structure of scales of *Latimeria chalumnae*, J. Zool. 167 (1972) 501–509.
[193] T.O.R. Orvig, Paleohistological notes I. On the structure of the bone tissue in the scales of certain Palaeonisciformes, Arkiv Zool. 10 (1957) 481–490.
[194] G.H. Roux, The microscopic anatomy of the *Latimeria* scale, S. Afr. J. Med. Sci. 7 (1942) 1–18.
[195] E. Jarvik, On some osteolepiform crossopterygians from the Upper Old Red Sandstone of Scotland, K. Svenska Vetenskapsakad. Handl. 2 (1950) 1–35.
[196] V.R. Sherman, W. Yang, M.A. Meyers, The materials science of collagen, J. Mech. Behav. Biomed. Mater. (2015) (in press).
[197] J.R. Grubich, S. Huskey, S. Crofts, G. Orti, J. Porto, Mega-bites: extreme jaw forces of living and extinct piranhas (Serrasalmidae), Sci. Report. (2012).
[198] P.-Y. Chen, J. Schirer, A. Simpson, R. Nay, Y.-S. Lin, W. Yang, M.I. Lopez, J. Li, E.A. Olevsky, M.A. Meyers, Predation versus protection: fish teeth and scales evaluated by nanoindentation, J. Mater. Res. 27 (2012) 100–112.
[199] A.K. Dastjerdi, F. Barthelat, Teleost fish scales amongst the toughest collagenous materials, J. Mech. Behav. Biomed. Mater. (2015) (in press).
[200] I.H. Chen, W. Yang, M.A. Meyers, Leatherback sea turtle shell: a tough and flexible biological design, Acta Biomater. (2015) (in press).
[201] J.D.R. Houghton, T.K. Doyle, J. Davenport, R.P. Wilson, G.C. Hays, The role of infrequent and extraordinary deep dives in leatherback turtles (*Dermochelys coriacea*), J. Exp. Biol. 211 (2008) 2566–2575.
[202] L. Besseau, Y. Bouligand, The twisted collagen network of the box-fish scutes, Tissue Cell 30 (1998) 251–260.
[203] C.-Y. Sun, P.-Y. Chen, Structural design and mechanical behavior of alligator (*Alligator mississippiensis*) osteoderms, Acta Biomater. 9 (2013) 9049–9064.
[204] S. Amini, A. Masic, L. Bertinetti, J.S. Teguh, J.S. Herrin, X. Zhu, H.B. Su, A. Miserez, Textured fluorapatite bonded to calcium sulphate strengthen stomatopod raptorial appendages, Nat. Commun. 5 (2014).
[205] J.C. Weaver, G.W. Milliron, A. Miserez, K. Evans-Lutterodt, S. Herrera, I. Gallana, W.J. Mershon, B. Swanson, P. Zavattieri, E. DiMasi, D. Kisailus, The stomatopod dactyl club: a formidable damage-tolerant biological hammer, Science 336 (2012) 1275–1280.
[206] J.D. Currey, A. Nash, W. Bonfield, Calcified cuticle in the stomatopod smashing limb, J. Mater. Sci. 17 (1982) 1939–1944.
[207] N. Guarín-Zapata, J. Gomez, N. Yaraghi, D. Kisailus, P.D. Zavattieri, Shear wave filtering in naturally-occurring Bouligand structures, Acta Biomater. 23 (2015) 11–20.
[208] L.K. Grunenfelder, N. Suksangpanya, C. Salinas, G. Milliron, N. Yaraghi, S. Herrera, K. Evans-Lutterodt, S.R. Nutt, P. Zavattieri, D. Kisailus, Bio-inspired impact-resistant composites, Acta Biomater. 10 (2014) 3997–4008.
[209] D.A.D. Parry, A.C.T. North, Hard alpha-keratin intermediate filament chains: substructure of the N- and C-terminal domains and the predicted structure and function of the C-terminal domains of Type I and Type II chains, J. Struct. Biol. 122 (1998) 67–75.
[210] J. McKittrick, P.-Y. Chen, L. Tombolato, E.E. Novitskaya, M.W. Trim, G.A. Hirata, E.A. Olevsky, M.F. Horstemeyer, M.A. Meyers, Energy absorbent natural materials and bioinspired design strategies: a review, Mater. Sci. Eng. C 30 (2010) 331–342.
[211] D. Raabe, A. Al-Sawalmih, S.B. Yi, H. Fabritius, Preferred crystallographic texture of alpha-chitin as a microscopic and macroscopic design principle of the exoskeleton of the lobster *Homarus americanus*, Acta Biomater. 3 (2007) 882–895.
[212] Y.S. Han, G. Hadiko, M. Fuji, M. Takahashi, Factors affecting the phase and morphology of $CaCO_3$ prepared by a bubbling method, J. Eur. Ceram. Soc. 26 (2006) 843–847.
[213] M.I. Lopez, M.A. Meyers, The organic interlamellar layer in abalone nacre: formation and mechanical response, Mater. Sci. Eng. C 58 (2015) 7–13.
[214] J.R. Young, M. Geisen, L. Cros, A. Kleijne, I. Probert, J.B. Ostergaard, A guide to extant coccolithophore taxonomy, J. Nanoplankton Res. 1 (2003) 1–132.
[215] G. Mayer, M. Sarikaya, Rigid biological composite materials: structural examples for biomimetic design, Exp. Mech. 42 (2002) 395–403.
[216] S. Weiner, L. Addadi, Design strategies in mineralized biological materials, J. Mater. Chem. 7 (1997) 689–702.
[217] B.H. Ji, H.J. Gao, Mechanical properties of nanostructure of biological materials, J. Mech. Phys. Solids 52 (2004) 1963–1990.
[218] I. Jager, P. Fratzl, Mineralized collagen fibrils: a mechanical model with a staggered arrangement of mineral particles, Biophys. J. 79 (2000) 1737–1746.
[219] J.F.V. Vincent, U.G.K. Wegst, Design and mechanical properties of insect cuticle, Arthropod Struct. Dev. 33 (2004) 187–199.
[220] G. De With, H.J.A. Van Dijk, N. Hattu, K. Prijs, Preparation, microstructure and mechanical properties of dense polycrystalline hydroxy apatite, J. Mater. Sci. 16 (1981) 1592–1598.
[221] C. Levi, J.L. Barton, C. Guillemet, E. Lebras, P. Lehuede, A remarkably strong natural glassy rod — the anchoring spicule of the monorhaphis sponge, J. Mater. Sci. Lett. 8 (1989) 337–339.
[222] M. Sarikaya, H. Fong, N. Sunderland, B.D. Flinn, G. Mayer, A. Mescher, E. Gaino, Biomimetic model of a sponge-spicular optical fiber — mechanical properties and structure, J. Mater. Res. 16 (2001) 1420–1428.
[223] P.-Y. Chen, A.Y.M. Lin, A.G. Stokes, Y. Seki, S.G. Bodde, J. McKittrick, M.A. Meyers, Structural biological materials: overview of current research, JOM 60 (2008) 23–32.
[224] A.P. Jackson, J.F.V. Vincent, R.M. Turner, The mechanical design of nacre, Proc. R. Soc. B 234 (1988).
[225] D.S. Fudge, J.M. Gosline, Molecular design of the alpha-keratin composite: insights from a matrix-free model, hagfish slime threads, Proc. R. Soc. B 271 (2004) 291–299.
[226] D.K. Hayes, W.D. Armstrong, Distribution of mineral material in calcified carapace and claw shell of the American lobster, *Homarus americanus*, evaluated by means of microroentgenograms, Biol. Bull. 121 (1961) 307–315.
[227] L.D. Mkukuma, J.M.S. Skakle, I.R. Gibson, C.T. Imrie, R.M. Aspden, D.W.L. Hukins, Effect of the proportion of organic material in bone on thermal decomposition of bone mineral: an investigation of a variety of bones from different species using thermogravimetric analysis coupled to mass spectrometry, high-temperature X-ray diffraction, and Fourier transform infrared spectroscopy, Calcif. Tissue Int. 75 (2004) 321–328.
[228] S. Sankar, S. Sekar, R. Mohan, S. Rani, J. Sundaraseelan, T.R. Sastry, Preparation and partial characterization of collagen sheet from fish (*Lates calcarifer*) scales, Int. J. Biol. Macromol. 42 (2008) 6–9.